JGR Biogeosciences

RESEARCH ARTICLE
10.1029/2019JG005414

Geochemistry of Small Canadian Arctic Rivers with Diverse Geological and Hydrological Settings

Kristina A. Brown[1,2], William J. Williams[2], Eddy C. Carmack[2], Greg Fiske[3], Roger François[4], Donald McLennan[5], and Bernhard Peucker-Ehrenbrink[1]

[1]Woods Hole Oceanographic Institution, Woods Hole, MA, USA, [2]Fisheries and Oceans Canada, Institute of Ocean Sciences, Sidney, British Columbia, Canada, [3]Woods Hole Research Center, Falmouth, MA, USA, [4]University of British Columbia, Vancouver, British Columbia, Canada, [5]Polar Knowledge Canada - Canadian High Arctic Research Station, Cambridge Bay, Nunavut, Canada

Key Points:
- Geochemical characteristics of Canadian Arctic Archipelago rivers reflect geological and hydrological heterogeneity across the region
- Time-series observations from two CAA rivers reveal weak, positive concentration-discharge relationships
- Major ion characteristics of CAA rivers are similar to large Arctic rivers, but their response to future change will likely differ

Supporting Information:
- Supporting Information S1
- Table S1
- Table S2
- Table S3
- Table S4

Correspondence to:
K. A. Brown,
kristina.brown@dfo-mpo.gc.ca

Citation:
Brown, K. A., Williams, W. J., Carmack, E. C., Fiske, G., François, R., McLennan, D., & Peucker-Ehrenbrink, B. (2020). Geochemistry of small Canadian Arctic Rivers with diverse geological and hydrological settings. *Journal of Geophysical Research: Biogeosciences*, *125*, e2019JG005414. https://doi.org/10.1029/2019JG005414

Received 6 AUG 2019
Accepted 25 DEC 2019
Accepted article online 2 JAN 2020

Abstract A survey of 25 coastal-draining rivers across the Canadian Arctic Archipelago (CAA) shows that these systems are distinct from the largest Arctic rivers that drain watersheds extending far south of the Arctic circle. Observations collected from 2014 to 2016 illustrate the influences of seasonal hydrology, bedrock geology, and landscape physiography on each river's inorganic geochemical characteristics. Summertime data show the impact of coincident gradients in lake cover and surficial geology on river geochemical signatures. In the north and central CAA, drainage basins are generally smaller, underlain by sedimentary bedrock, and their hydrology is driven by seasonal precipitation pulses that undergo little modification before they enter the coastal ocean. In the southern CAA, a high density of lakes stores water longer within the terrestrial system, permitting more modification of water isotope and geochemical characteristics. Annual time-series observations from two CAA rivers reveal that their concentration-discharge relationships differ compared with those of the largest Arctic rivers, suggesting that future projections of dissolved ion fluxes from CAA rivers to the Arctic Ocean may not be reliably made based on compositions of the largest Arctic rivers alone, and that rivers draining the CAA region will likely follow different trajectories of change under a warming climate. Understanding how these small, coastal-draining river systems will respond to climate change is essential to fully evaluate the impact of changing freshwater inputs to the Arctic marine system.

Plain Language Summary River inputs are important for the physics and biogeochemistry of the rapidly changing Arctic Ocean. Most of our knowledge of river inputs comes from studies of the six largest rivers which drain areas reaching far south of the Arctic Circle, omitting 45% of the pan-Arctic watershed. This has left a gap in our understanding of smaller, coastal-draining rivers and how these are influenced by the changing climate. We studied 25 coastal-draining rivers in the Canadian Arctic Archipelago (CAA) for geochemical comparison to the larger, more southerly rivers. Summertime survey data show that geochemical properties change from south to north following the distribution of lake cover, bedrock geology, and glacial history. Unlike the largest Arctic rivers, however, repeat observations over the annual cycle indicate that dissolved ion concentrations are not strongly influenced by changing water fluxes in the CAA region. To fully understand the impact of changing freshwater inputs to the Arctic Ocean requires consideration of smaller watersheds that may change differently compared to the largest Arctic rivers.

1. Introduction

Increased precipitation, river runoff, and permafrost thaw have been observed throughout the pan-Arctic region over the past decades, contributing to an increased flux of freshwater and land-derived material to the ocean (e.g., Doxaran et al., 2015; Peterson et al., 2002; Romanovsky et al., 2013; White et al., 2007; Zhang et al., 2008). These changes to the Arctic freshwater system will dictate the future state of the Arctic marine environment (e.g., Carmack et al., 2016), making their characterization across space and time critical to predicting Arctic Ocean change. Runoff via Arctic rivers accounted for between 40% and 49% of the total influx of freshwater to the Arctic Ocean over the 10-year period of the 2000s, exceeding precipitation (20–27%), Bering Strait flow through (25–31%), and inputs from the Greenland ice sheet (3–5%; Haine et al., 2015). Much of what we know about the riverine response to Arctic environmental change comes from over a decade of observations of the six largest Arctic rivers by the Pan-Arctic River Transport of

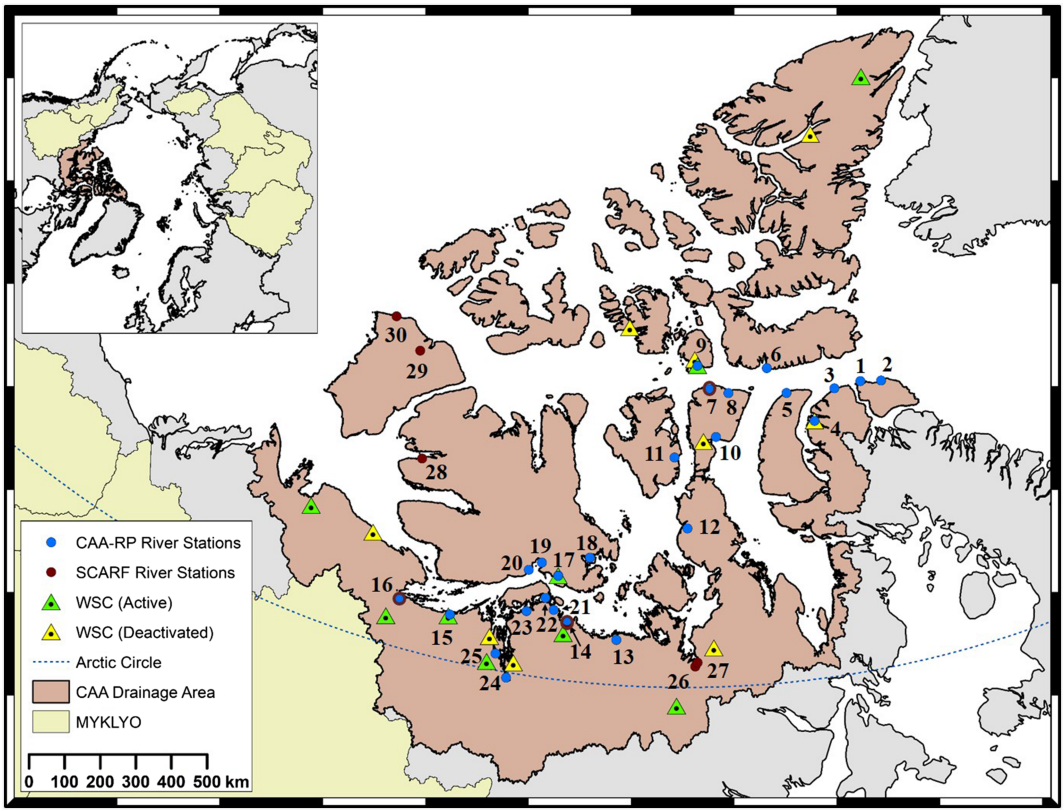

Figure 1. The Canadian Arctic Archipelago (CAA) drainage region (brown), in comparison to the pan-Arctic watersheds of the six major Arctic rivers, clockwise from the CAA: Mackenzie, Yukon, Kolyma, Lena, Yenisei, and Ob' (MYKLYO, lime shading, inset). Active (green) and deactivated (yellow) Water Survey of Canada (WSC) gauge locations are indicated with triangles. The locations of marine-terminating rivers visited in this study are numbered 1–25 (blue dots), with locations 26–30 added from Alkire et al. (2017) (red dots), three rivers (7, 14, and 16) were included in both studies. Rivers sampled include [1] Akpat Kuunga*; [2] Glacier River*; [3] Charles York River; [4] Marcil Creek; [5] Saaqu River; [6] Devon Island*; [7] Cunningham River; [8] Garnier River; [9] Mecham River; [10] Creswell River; [11] Le Feuvre Inlet*; [12] Pasley River; [13] Simpson River; [14] Ellice River; [15] Tree River; [16] Coppermine River; [17] Freshwater Creek; [18] Jayko River; [19] Ekalluk River; [20] Halokvik River; [21] Tingmeak River; [22] Elu Inlet*; [23] Koignuk River; [24] Western River; [25] Burnside River; [26] Back River; [27] Hayes River; [28] Kuujuua River; [29] Thomsen River; and [30] Karasok River; with time-series observations collected from the Coppermine River [16] and Freshwater Creek [17] from 2014 to 2016. Maps are displayed using the Canadian Albers Equal Area projection. Rivers denoted with an * had no official name on available charts so were named according to distinctive features of the region.

Nutrients, Organic Matter, and Suspended Sediments (PARTNERS) and Arctic Great Rivers Observatory (Arctic-GRO) programs (e.g., Holmes et al., 2002; McClelland et al., 2004; Peterson et al., 2002; Peterson et al., 2006; White et al., 2007) that have established a necessary benchmark against which to measure future change (e.g., Holmes et al., 2011; Holmes et al., 2013; McClelland et al., 2006; McClelland et al., 2008). These six large systems, the Kolyma, Lena, Mackenzie, Ob', Yenisei, and Yukon rivers, account for over 55% of river discharge into the Arctic Ocean (e.g., Holmes et al., 2013; Haine et al., 2015); however, their expansive drainage basins extend far south of the Arctic Circle (Figure 1) and the Westerly storm tracks, and thus their geochemical characteristics can be strongly affected by warming impacts on temperate latitudes. This focus on the largest Arctic rivers leaves a significant knowledge gap in the biogeochemical data record for smaller river systems within the high-latitude continuous permafrost zone, especially along the coastal margins (e.g., Bring & Destouni, 2009; Holmes et al., 2012) and in the regions far away from the largest river inputs. Recent estimates indicate that these smaller ($<0.1 \times 10^6$ km^2; <30 km^3 year^{-1}), coastal-draining systems could account for 20–30% of the river discharge entering the Arctic Ocean annually (Haine et al., 2015; Holmes et al., 2013). This lack of data limits a deeper understanding of many important Arctic biogeochemical processes in higher latitude regions that are both particularly vulnerable to change (e.g., Carmack et al., 2016; Schuur et al., 2008; Schuur et al., 2015) and predicted to respond more strongly to the increased warming (Bring et al., 2017).

Smaller river systems that discharge directly into the Arctic Ocean drain approximately 22% of the pan-Arctic watershed (Holmes et al., 2013), but the number of reliable discharge stations covering this area is very small, with those that do exist also on the decline (Laudon et al., 2017). Available long-term discharge records have been compiled for at least 30 "small" ocean-terminating river systems across the pan-Arctic (R-ArcticNet catalogue, Lammers et al., 2016; Environment Canada, Li Yung Lung et al., 2018), but coverage along the Alaskan coast (four rivers) and Canadian coast (eight rivers) is limited. Several regional studies have also described geochemical variables from "small" coastal-draining rivers in the White Sea (Kem' River, Shevchenko et al., 2005; Mezen and Onega rivers, Dittmar & Kattner, 2003; Holmes et al., 2000), the Alaskan Beaufort Sea (Colville, Sagavanirktok, and Kuparuk rivers; Holmes et al., 2008; McClelland et al., 2014), and the Canadian Arctic Archipelago (CAA; Alkire et al., 2017; Lafrenière & Lamoureux, 2008; Lewis et al., 2012; Li Yung Lung et al., 2018), but few include sufficient data to assess regional changes over time, nor do they include the necessary ancillary information to allow comparison with the largest Arctic river systems.

The CAA's high Arctic islands and bordering mainland, which alone comprise a shoreline of over 100,000 km, offer a unique opportunity to investigate and characterize small rivers directly draining into the Arctic Ocean. The entire CAA drainage area extends from just below the Arctic Circle to Canada's northernmost point on Ellesmere Island (Figure 1), providing a semicontinuous gradient of high Arctic landscapes across almost 20° of latitude. South-north variation in vegetation (CAVM, 2003), soil type (Hugelius et al., 2013), bedrock geology (Garrity & Soller, 2009), and lake cover (Messager et al., 2016) provide a backdrop against which comparisons between individual rivers may be used to investigate the influence of regional landscape characteristics on the land-to-ocean delivery of inorganic ions. Furthermore, the CAA land area is comparable to that of the largest North American Arctic river watersheds (CAA: 1,471,410 km^2; Mackenzie: 1,780,000 km^2; Yukon: 830,000 km^2; Holmes et al., 2012) but contributes freshwater and terrigenous inputs to a much smaller, geographically confined marine system of channels, basins, and tidal straits (Figure 1). This makes the CAA continental shelf a potentially important region for geochemical modification as Arctic Ocean and Pacific-origin waters exit into the North Atlantic via Baffin Bay (e.g., McLaughlin et al., 2006; Shadwick et al., 2011).

This study presents new geochemical observations from a broad survey of 25 coastal-draining rivers throughout the CAA, including 20 rivers systems with no previously published geochemical data. We also present high-resolution time series from two river systems in the southern CAA, each draining different, representative bedrock types, to provide seasonal context for summertime survey observations and to permit comparison of smaller CAA rivers to the largest Arctic river systems. We use these data to investigate the influence of landscape-scale controls (e.g., hydrology, bedrock geology, and landscape physiography) on river geochemical composition. These analyses reveal the dominant influence of spatial gradients in landscape characteristics in dictating the geochemical composition of each river; we further speculate as to the trajectory of change of these systems under a warming Arctic climate.

2. Methods

CAA rivers were sampled during the summer season, from 1 August to 9 September 2014, and 11–15 August 2015, with access via various modes of transportation (supporting information, Table S1) as part of the Canadian Arctic Archipelago Rivers Program (CAA-RP) and the Canadian Arctic GEOTRACES program. Here we report summer observations collected from 25 different rivers (Figure 1), as well as annual time-series observations from the Coppermine River in Kugluktuk, Nunavut (NU) (5 August 2014 to 23 August 2016) and time-series observations during the open-water season from Freshwater Creek in Cambridge Bay, NU (19 June 2014 to 16 September 2016). Lake samples were also collected opportunistically during float plane air surveys in 2014 and 2015 as part of the CAA-RP study in the southern CAA. River water samples were collected according to methods developed by the Arctic-GRO (http://www.arcticgreatrivers.org/), as described in detail in Supporting Information S1.1; lake sampling followed the same general methods, with collection carried out in deeper waters away from the shore. Basic sample collection and analytical methods are described below.

2.1. Sample Collection

2.1.1. River and Lake Water Sample Collection

At each site, water was collected using prerinsed 60-ml syringes (Fisher Scientific) directly from just below the surface or by first pumping water through a 0.45-μm cartridge filter (Farrwest Environmental Supply) using a peristaltic pump (Pegasus Athena). Water collected for geochemical analyses of dissolved constituents was filtered through 0.22-μm Sterivex cartridges (Millipore) into triply rinsed 4-ml amber glass vials (Wheaton) for stable water isotope analyses and 125-ml HDPE bottles (Fisher Scientific) for determination of dissolved major and minor element concentrations. Dissolved ion and stable water isotope samples were stored in the dark at room temperature or refrigerated until analyses. At most sites, hydrographic measurements were collected using either an RBR-CTD (Ruskin Scientific) or a CastAway-CTD (SonTek).

Samples for the determination of dissolved inorganic carbon (DIC) and total alkalinity (TA) were collected either by (1) submerging prerinsed 250-ml borosilicate glass bottles (Pyrex) below the water surface (2014), or (2) by using a Niskin sampling bottle fixed to a line and closed with a messenger-weight from the side of the vessel (2014), or (3) by pumping river water through a 0.45-μm cartridge filter (Farrwest Environmental Supply) using a peristaltic pump (Pegasus Athena) into 250-ml borosilicate glass reagent bottles (Pyrex) (2015). Bottles were allowed to overflow at least one full bottle volume, and headspace was adjusted to ~1% of the sample volume before being preserved with a saturated solution of $HgCl_2$ and stoppered with greased (silicon-free high-vacuum grease, Apiezon Type-M) ground glass stoppers (held in place with elastic bands or vinyl electrical tape [3 M]) and then stored in an cool, dark, insulated box.

Samples for the determination of salinity were collected in parallel with carbonate system samples, using the same three collection methods described above. Glass bottles (200 ml) and caps were rinsed three times before filling, then capped with a plastic insert followed by a screw-on cap (after McLaughlin et al., 2012).

2.1.2. Rain Sample Collection

Precipitation was collected during two significant rain events. On 25 August 2015, overnight precipitation was collected into an HCl cleaned plastic shoe box (The Container Store) placed on a stack of pallets in an open lot in the center of the community of Kugluktuk, NU (67.8276°N, −115.1015°E). Another rain sample was collected on 20 August 2016 from overnight precipitation in the community of Cambridge Bay, NU (69.12°N, −105.04°E) using the same collection box placed on an open porch at the newly built Canadian High Arctic Research Station accommodations. In both cases, rain samples were processed immediately the following morning in order to limit the influences of evaporation. Collected rain was processed in the same manner as river water samples.

2.2. Analytical Geochemical Methods

Analytical methods used in this study for the determination of geochemical concentrations are well established. Dissolved cation (Ca, Na, Mg, K, Sr, Ba) and anion (Cl, SO_4) analyses were conducted at WHOI laboratories following the methods outlined in Voss et al. (2014), with analytical uncertainty of ±5% (generally better than ±2%) and ±3%, respectively. Oxygen and hydrogen stable isotope composition of water ($\delta^{18}O$, $\delta^{2}H$) were determined at Brown University with analytical precision of ±0.1‰ and ±1‰, respectively. Dissolved organic carbon (DOC) concentration was determined at the Woods Hole Research Center using a Shimadzu high-temperature TOC-V analyzer following Holmes et al. (2012; Student Partners Program) with an overall analytical precision of <5% (Mann et al., 2012). Analytical methods are described in detail in Supporting Information S1.2.

Components of the inorganic carbon system (DIC, TA) were determined either at the Institute of Ocean Sciences (Sidney, B.C.) or aboard the CCGS Louis S. St. Laurent following Dickson et al. (2007), as described in detail in Supporting Information S1.2. Both DIC and TA were calibrated against certified reference materials provided by Andrew Dickson (Batch 133 and 138 for 2014 and 2015, respectively, Scripps Institute of Oceanography). Pooled standard deviation (Sp; IUPAC, 1997) of duplicate analyses for DIC ($n = 20$) and TA ($n = 20$) were ±4.0 μmol kg^{-1} and ±3.0 μmol kg^{-1}.

Salinity was determined either at the Institute of Ocean Sciences (Sidney, BC) or aboard the CCGS Louis S. St. Laurent using a Guildline Autosalinometer (Autosal) Model 8400B (SN: 68572 or 69086, respectively) referenced against IAPSO Standard Seawater (OSIL, batch P156 and P157 for 2014 and 2015, respectively) as described in McLaughlin et al. (2012). Salinity is reported on the Practical Salinity Scale 1978 (PSS78).

2.3. Charge Balance Assessment

Bicarbonate (HCO_3^-) and carbonate (CO_3^{2-}) concentrations were determined in river samples using average measured values of DIC, TA, and salinity in the Excel version of CO2Sys (Pierrot et al., 2006). Calculations were made using the carbonic acid dissociation constants, K1 and K2 for freshwater (salinity = 0) by Millero (1979), dissociation constants for $KHSO_4$ determined by (Dickson, 1990), and Total Boron from Uppström (1974). As temperature was not determined in every river, an average temperature of 8.5 °C ($n = 15$) was used in all calculations. River temperatures followed a latitudinal gradient, with the lowest values in the central CAA (Glacier River, 2.5 °C) and highest in the south (Coppermine River, 13.3 °C). For rivers where temperature was recorded, recalculating HCO_3^- and CO_3^{2-} using measured values resulted in less than a 1% difference from calculations using the average temperature (8.5 °C). Charge balance error (after Alkire et al., 2017) was then determined for river samples where major ion and inorganic carbon species (HCO_3^- and CO_3^{2-}) were available (Table S2). The average charge balance error for all of our river samples of ±2% of the total charge is within the reported analytical uncertainty of our measurements.

2.4. GIS Methods

Watershed boundaries for each river were derived from Canadian digital elevation model (DEM) data provided by Natural Resources Canada (http://geogratis.gc.ca/) and, where possible, were cross-checked against available Water Survey of Canada (WSC) drainage basin definitions for gauged rivers in the study region (Coppermine River, Freshwater Creek, Ellice River, and Back River). We note that errors in the determination of these drainage basins can arise due to the coarseness of the available DEM at the time of this study. From these watershed deliniations the predominant bedrock lithologies were quantified following the methods outlined in Peucker-Ehrenbrink and Miller (2003, 2007) using the digital maps of North American bedrock geology at 1:5,000,000 (Garrity & Soller, 2009). Watershed boundaries were also used to determine the percent coverage of lakes within each river drainage basin from the HydroLAKES (v10) data set, which describes the characteristics and abundance of a global data sets of natural lakes and human-made reservoirs with a surface area of 0.1 km^2 or greater (Messager et al., 2016). Surficial geology characteristics of each drainage basin were determined using the Surficial geology of Canada, Canadian Geoscience Map 195, scale 1:5,000,000 (Geological Survey of Canada, 2014).

The CAA drainage region illustrated in Figure 1 was defined using the USGS HYDRO1k North American data set (Levels 5 & 6) which is a product of the 30 arc-second DEM of the world (GTOPO30), available from https://doi.org/10.5066/F77P8WN0. As with determinations for individual rivers, the coarseness of the available DEM may contribute to errors in the determination of the limits of the CAA drainage region. To estimate the average annual discharge from the CAA drainage region, we used historical WSC flow gauge data from 18 marine-terminating rivers (Figure 1) and determined the relationship between average annual discharge and drainage basin area following Prowse and Flegg (2000; see Supporting Information S2). Based on our definition of the CAA drainage region (Figure 1), we estimate the total drainage area at 1,471,410 km^2 with a corresponding average annual discharge of 250 $km^3\ year^{-1}$ (Supporting Information S2). These values are within the range of previous studies (see Supporting Information S2) and on the same order as the Mackenzie and Yukon rivers (316 and 208 $km^3\ year^{-1}$, respectively; Holmes et al., 2012). We use these determinations to further compare the geochemical observations from this study to those of the major Arctic rivers.

2.5. Discharge Data

Historical daily discharge (flow) data were accessed from the Environment Canada (EC) HYDAT Database National Water Data Archive using their EC Data Explorer v2.1 with hydrometric and station information data provided by the WSC, release edition: 18 October 2016 (HYDAT, 2016). Preliminary daily average discharge data for the Coppermine River and Freshwater Creek in 2016 were provided by EC. We note that EC was unable to fill gaps in the data records for these two rivers over our study period (2014–2016) due to lack of measurements. We chose two different approaches to fill data gaps in these two rivers as described in Supporting Information S1.3. Data gaps in the Coppermine River record accounted for less than 27% of the 2015 and 2016 annual records, whereas Freshwater Creek had an 8% data gap in the 2014 record. Resolving these gaps with linear interpolation matched well with the historical data records for both rivers; however, it should be noted that these estimates represent averaged scenarios and should be extrapolated

with caution. Future reevaluation of discharge data from these years is welcome and can be used to further evaluate this approach once these data are available.

2.6. Geochemical Flux Determination

Geochemical fluxes of dissolved ions, DOC, and flow-weighted concentrations of stable isotopes were determined for the Coppermine River and Freshwater Creek using LoadRunner v 1.2b (Booth et al., 2007). This program was developed to automate analyses of the USGS program LOADEST, which applies a best fit model to compute geochemical fluxes as a function of discharge (Runkle et al., 2004). We followed the approach of Tank et al. (2012) to determine the fit of time-series observational data for each major ion using the adjusted maximum likelihood estimate (Cohn, 1988; Cohn et al., 1992; Table S4). Freshwater Creek presented a particular challenge to model, as this river freezes solid for almost 7 months of the year (November–May), resulting in LOADEST-modeled concentrations being extrapolated disproportionally high at the lowest flow days during the onset of melt and freeze-up. To mitigate this modeling issue, we used monthly average concentration data from the LOADEST outputs to calculate discharge-weighted ion concentrations and fluxes from Freshwater Creek. This gave modeled ion concentrations that fell within measured values in the river, instead of fivefold to tenfold higher as was determined using the daily estimates. For both the Coppermine River and Freshwater Creek we used the WSC daily discharge data as described in section 2.5. LOADEST model fit parameters and regression statistics are presented in Table S4. To increase the resolution of the Coppermine River geochemical data set, observations from 2014 to 2015 presented in Alkire et al. (2017) were combined with our observations to determine LOADEST-modeled average ion concentrations and annual fluxes.

For modeled ion concentrations and fluxes from Arctic-GRO rivers, we used LOADEST-derived daily concentrations data for Ca, Na, Mg, Cl, Sr, and SO_4 for the period 2000–2009 determined by Tank et al. (2012) (available from the Arctic Data Center; Peterson et al., 2016). To expand the comparison to all of the ions in our study, we computed daily loads and concentrations of K and Ba over the 2000–2009 interval with LOADEST using observations made during the PARTNERS program (2003 to 2006) following the methods outlined in Tank et al. (2012) and Holmes et al. (2012). We linearly interpolated to fill any gaps within the Arctic-GRO discharge data set and followed Tank et al. (2012) conventions to correct for temporal offsets between sampling and gauging locations. Daily average loads and ion concentrations determined in LOADEST were then discharge-weighted using data from the Arctic-GRO discharge data, and an annual average was computed for the model interval (2000–2009), also following the methods of Tank et al. (2012).

2.7. Scaling Approaches

To determine the broader pan-Arctic influence of CAA rivers, we attempt to scale observations from this study and those of Alkire et al. (2017), which, combined, characterize a drainage area of about 16% of the CAA (240,442 km^2 of the estimated 1,471,410 km^2 total, as defined in Figure 1). Three rivers (Cunningham, Ellice, and Coppermine) were included in both studies, but the addition of the Back and Hayes rivers from Alkire et al. (2017) increases the total drainage region covered by 112,000 km^2. The Halokvik, Kuujuua, Thomsen, and Karasok rivers were not included in the scaling analyses as drainage basin definitions were not available. We apply two approaches to scale individual river observations to the CAA drainage region to estimate discharge-weighted constituent concentrations and annual fluxes to the ocean. First, we use an "end-member" approach (CAA-EM; section 2.7.1) that is similar to the approach of Alkire et al. (2017) based on bedrock geology distributions across the CAA. Second, we use an "area-weighted" approach (CAA-AW; section 2.7.2) that linearly scales constituent concentrations based on drainage area. Since average annual discharge and drainage basin area were tightly correlated in EC monitored CAA rivers (Figure S1), the CAA-AW approach essentially mimics a discharge-weighted estimate for constituent concentrations. We then compare these two approaches to constituent concentration and flux estimates generated for the six largest Arctic rivers with the Coppermine River and Freshwater Creek.

2.7.1. "End-Member" Approach (CAA-EM)

Here we define the average geochemical characteristics of different bedrock types across the CAA. As our geology data set is separated into the categories of "intrusive, metamorphic, sedimentary, and volcanic" bedrock (Garrity & Soller, 2009), we have chosen representative "end-member" drainage systems that are dominated by these bedrock types (Table S2). We used the drainage basin of the river at Elu Inlet as representative of intrusive bedrock (100%; #22), the Koignuk River for volcanic bedrock (55%; #23), and the area-weighted

Table 1
Geochemical Characteristics of CAA Rivers and the "Big 6" Arctic Rivers.

	CAA-RP (this study)	SCARF[a]	Arctic-GRO[b] "Big 6"
Calcium (μM)	54.0 to 1,174	14.3 to 873	189 to 1,619
Magnesium (μM)	22.7 to 1,632	13.0 to 572	60.5 to 562
Sodium (μM)	18.3 to 2,514	18.4 to 496	29.1 to 2,244
Potassium (μM)	2.87 to 63	6.20 to 567	7.30 to 53
Sulphate (μM)	13.3 to 562	7.3 to 1,218	11.0 to 195
Chloride (μM)	9.5 to 2,810	26.0 to 389	1.6 to 2,297
Strontium (nM)	71 to 4,471	47 to 1,152	469 to 4,253
Barium (nM)	16.3 to 430	4.5 to 255	63 to 371[c]
$\delta^{18}O\text{-}H_2O$ (‰)	−24.5 to −16.9	−25.6 to −17.0	−25.6 to −3.4
$\delta^{2}H\text{-}H_2O$ (‰)	−185 to −136		−198 to −97
DIC (μmol kg^{-1})	147 to 2,252		
TA (μmol kg^{-1})	93 to 2,272	58 to 1,810	449 to 1,707[c]
DOC (mg C L^{-1})	0.2 to 14.6	0.6 to 6.9	1.0 to 24.6
Estimated average annual discharge of ALL river systems sampled (km^3 $year^{-1}$)	21	33	2,348[d]

[a]SCARF data from Alkire et al. (2017), our comparison only includes rivers that drain into the CAA directly: Back, Cunningham, Ellice, Hayes, Karasok, Kuujuua, and Thomson rivers. [b]Geochemical observations and daily average discharge measurements for each river taken from the Arctic-GRO data set edition 20151021 unless otherwise noted, including the Kolyma, Lena, Mackenzie, Ob', Yenisei, and Yukon rivers sampled as part of the PARTNERS and Arctic-GRO programs from 2003 to 2014. [c]Range of flow-weighted averages reported from Cooper et al. (2008). [d]Holmes et al. (2012).
Abbreviations: CAA-RP = Canadian Arctic Archipelago Rivers Program; DIC = dissolved inorganic carbon; DOC = dissolved organic carbon; PARTNERS = Pan-Arctic River Transport of Nutrients, Organic Matter, and Suspended Sediments; TA = total alkalinity.

average of the Simpson and Tingmeak rivers for metamorphic bedrock (69%; #13 & 21). To represent the sedimentary bedrock "end-member" we combined ten drainage basins with 100% coverage of sedimentary bedrock (#4–9, 11, 17–19) into an area-weighted average value.

Average dissolved ion concentrations from each of these "end-members" were then scaled to the total area of that bedrock type across the CAA. The bedrock composition for the entire CAA is glacial ice (5%), volcanic rocks (6%), intrusive rocks (9%), metamorphic rocks (15%), and sedimentary rocks (66%). In contrast, the river basins included in our study regions are underlain by volcanic rocks (3%), intrusive rocks (17%), metamorphic rocks (13%), and sedimentary rocks (67%). Our observations are therefore biased in favor of intrusive rocks and against regions covered in glacial ice (northern CAA) but otherwise match the broader CAA bedrock composition fairly well. Annual fluxes were then estimated by multiplying CAA-scaled constituent concentrations by the average annual discharge (250 km^3 $year^{-1}$; section 2.4).

2.7.2. Area-Weighted Approach (CAA-AW)

Here we linearly scale individual river observations to the CAA drainage area. An area-weighted average dissolved ion concentration value was determined using observations from all the CAA rivers noted above, with their contributions weighted by their drainage basin size (Table S2). These "area-weighted" average dissolved ion concentrations are then scaled linearly to the estimated size of the CAA drainage region and annual fluxes were estimated by multiplying by the average annual discharge (250 km^3 $year^{-1}$; section 2.4).

3. Results

3.1. General Geochemical Observations from the CAA Rivers Program

River dissolved composition reflects hydrology (section 3.2) and the balance of rock material weathering (section 3.3) within the drainage system. Dissolved ion concentrations varied by at least a factor of 15 to as much as 300 across the study region (Tables 1 and S2). In spite of this wide range of geochemical observations, some trends stand out. Dissolved concentrations of Cl and Na varied linearly ($r^2 = 0.99$, not shown), with Cl almost always in excess by an average factor of 1.2. Dissolved Cl concentrations in local rain water samples were almost twice those of Na, though overall the chemical composition of rain collected in Kugluktuk and Cambridge Bay during the study was quite different (Table S2). High concentrations of

SO_4 and Ca were coincident in four rivers (river #s 7, 8, 9, 10; Table S2); however, no relationship was observed for rivers with Ca concentrations less than 200 μM (not shown). Notably high concentrations of inorganic carbon (DIC, TA) were found in rivers draining the central CAA (#11, 12), which were as high as concentrations found in nearby marine waters (this study). The Burnside River (#25) and the Glacier River (#2) exhibited some of the lowest dissolved ion concentrations compared with the other rivers, whereas Le Feuvre Inlet (#11) had the highest concentrations for most constituents (Table S2). Regional survey observations from this study yield drainage basin area-weighted average concentrations of anions: Cl (257 μM), SO_4 (42 μM); cations: Ca (220 μM), Mg (170 μM), Na (224 μM), K (15.3 μM), Sr (279 nM), Ba (93 nM); and dissolved carbon: DIC (533 μmol kg^{-1}), TA (565 μmol kg^{-1}), DOC (4.0 mg C L^{-1}) that skew towards the lower end of concentration ranges measured for the region (Table 1).

Notably, the collection of CAA rivers sampled in this study exhibit quite high concentrations of Ca, Mg, and Na compared with those reported in Alkire et al. (2017), Table 1. Our values are within ranges seen in the larger Arctic rivers, except for Mg which was high even for the pan-Arctic data set. The highest Mg values were observed in Freshwater Creek, with the highest concentrations measured in early spring (June) and later in the season (September). If Freshwater Creek is removed from the data set, the highest Mg values observed do not exceed 677 μM, more similar to the other Arctic river data (Table 1). Both Sr and K concentrations also stand out, with observed K concentrations much lower than in the rivers sampled by Alkire et al. (2017); however, their high K values were observed in rivers on the western side of Victoria and Banks Islands, regions not sampled in our study. High concentrations of dissolved Sr were observed in the north and central CAA rivers from this study; in particular rivers sampled on Devon Island (#6) and Summerset Island (Creswell R., #10) which had values almost four times higher than observed by Alkire et al. (2017). Barium concentrations from northern Baffin Island (Charles York R., #3) were also high compared with other CAA observations and were more than 45% higher than the next highest river measured in this study (Marcel Creek, #4).

3.2. Hydrology: Stable Water Isotopes

Stable isotope ($\delta^{18}O$ and $\delta^{2}H$) signatures of CAA river water at the time of sampling fall along or below the global meteoric water line (GMWL; as defined in Clark & Fritz, 1997). Smaller catchments in the north and central CAA (open circles labeled 1–8, Figure 2a) were more closely associated with the GMWL (*d-excess* from 2 to 11; calculated after Dansgaard, 1964), whereas stable water isotope ratios of rivers draining the central to the southern CAA plot below the GMWL (open circles labeled 9–12, Figure 2a; *d-excess* from −2 to +2). Rivers in the Southern CAA (filled circles, Figure 2a) including the Coppermine River (triangles, Figure 2a) and Freshwater Creek (diamonds, Figure 2a), diverge even further from the GMWL, as do collected lake samples (asterisks, Figure 2a). Regional trends show *d-excess* decreases with longitude, from west to east ($r^2 = 0.80$; not shown) and latitude, south to north ($r^2 = 0.74$; not shown), consistent with the long-term cross-continent variation in $\delta^{18}O$ of precipitation (Gibson et al., 2005).

Time-series observations collected in the Coppermine River and Freshwater Creek show changing patterns of $\delta^{18}O$ over the seasonal flow cycle (Figure 2b shows $\delta^{18}O$ values, but $\delta^{2}H$ values follow similar trends). For the perennial Coppermine River, high discharge in the spring associated with ice breakup is marked by a pulse of isotopically light $\delta^{18}O$ values (Figure 2b, triangles). Freshwater Creek, which flows only after lake and river ice begins to melt, shows a much more pronounced light-isotope pulse with the initial breakup (Figure 2b, diamonds), rebounding towards higher (isotopically heavier) $\delta^{18}O$ values within a few days after the first observable flow. The stable isotopic signatures in both rivers become isotopically heavier as discharge increases with the advance of freshet and plateau near their highest values by the end of the open-water season. Stable isotope signatures of the Coppermine River remain nearly constant over winter while the river is ice-covered.

3.3. Geology: Major Ions

Dissolved major ion concentration ratios (Mg/Na vs. Ca/Na, in molar units) illustrate the influence of a diversity of bedrock types on river source waters, from igneous rocks to sedimentary rocks rich in carbonates (Figure 3). Bicarbonate to calcium ratios were generally elevated above 2:1 (average $HCO_3^-/Ca = 2.4$), indicating a mix of weathering products from both silicate and carbonate sources (not shown). Likewise, TA/Na reinforced trends seen in Mg/Na when plotted against Ca/Na (not shown). As indicated by Figure 3,

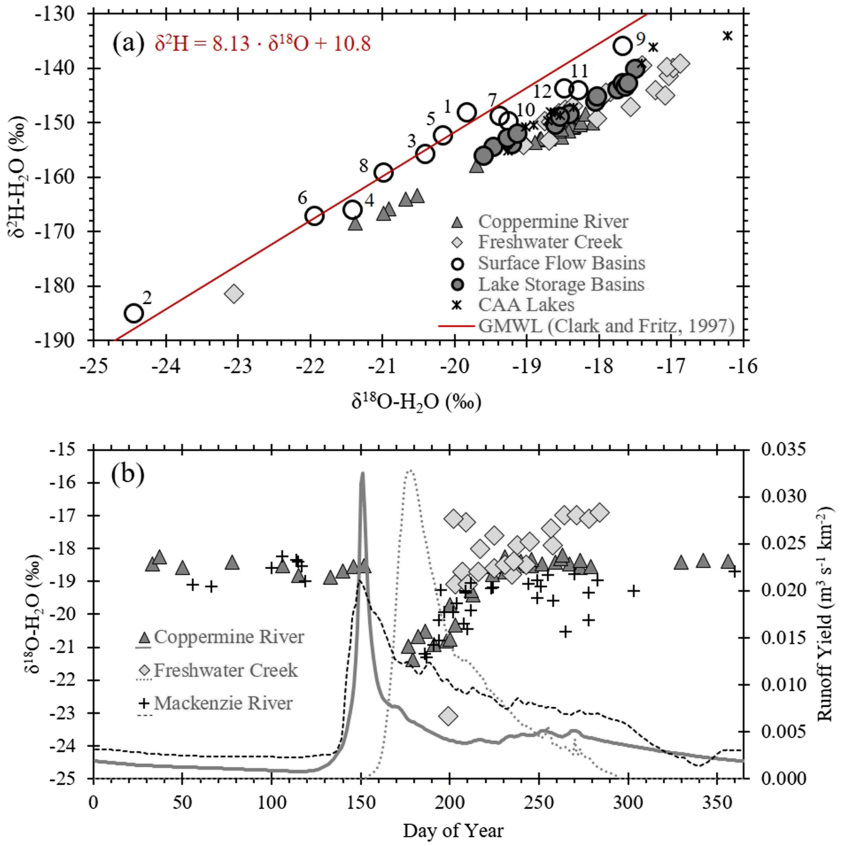

Figure 2. (a) Stable isotope ratios of water ($\delta^{18}O$, $\delta^{2}H$) in river (circles) and lake (asterisks) samples collected throughout the CAA and from time-series sampling in the Coppermine River (triangles) and Freshwater Creek (diamonds). Numbers refer to river names as in Figure 1. Isotope values that generally follow the GMWL (red line; Clark & Fritz, 1997) are termed SFD type (open circles), whereas those that move farther off the line are termed LSD type (filled circles). (b) Time-series observations of $\delta^{18}O$ from the Coppermine River (triangles), Freshwater Creek (diamonds), and Mackenzie River (crosses) illustrate the transition from snowmelt source waters during peak discharge (more depleted in ^{18}O) to lake flow the rest of the year (less depleted in ^{18}O). Single year examples of each river's annual runoff yield curve (daily average discharge/drainage basin area) are plotted for the Coppermine River (2014; solid gray line), Freshwater Creek (2015; dotted gray line), and Mackenzie River (2013; dashed black line). Mackenzie River time-series data are from the Arctic-GRO and PARTNERS programs (http://www.arcticgreatrivers.org/; dataset edition 20151021 with observations from June 2003 to June 2014).

drainage basin bedrock geology is quite variable throughout the sampling region (Figure 4). Watersheds draining predominantly sedimentary bedrock are found throughout the northeast and central CAA, in particular on Devon Island (#6), Summerset Island (#7, 8, 10), Boothia Peninsula (#12), and Victoria Island (#17–20). Whereas regions of metamorphic and intrusive bedrock are found in the southwestern CAA and on Bylot Island (#2), these drainage systems also include some volcanic bedrock. As expected, carbonate rock associated parameters (Ca, HCO_3^-, TA, DIC), followed the general trends in sedimentary bedrock distribution, with the highest concentrations associated with rivers draining 100% sedimentary bedrock (Table S2). Although there is no clear trend across the region, the highest Mg and Ba concentrations were measured in Victoria Island rivers (#17–20), which also drain 100% sedimentary bedrock.

3.4. Inorganic Flux Time Series: Coppermine River and Freshwater Creek

Although the linear relationships of log-log C-Q plots are weak, concentrations of Ca, Mg, Na, Cl, and Ba measured in the Coppermine River tended to increase with increasing discharge over the 2014–2016 time series (triangles, Figures 5 and S2). Notable exceptions are K, Sr, and SO_4 which show almost no change as discharge increases (Figures 5 and S2). There is much more scatter in the Freshwater Creek time series. Although ion concentrations look to increase with discharge in some cases, any trends are weak and in

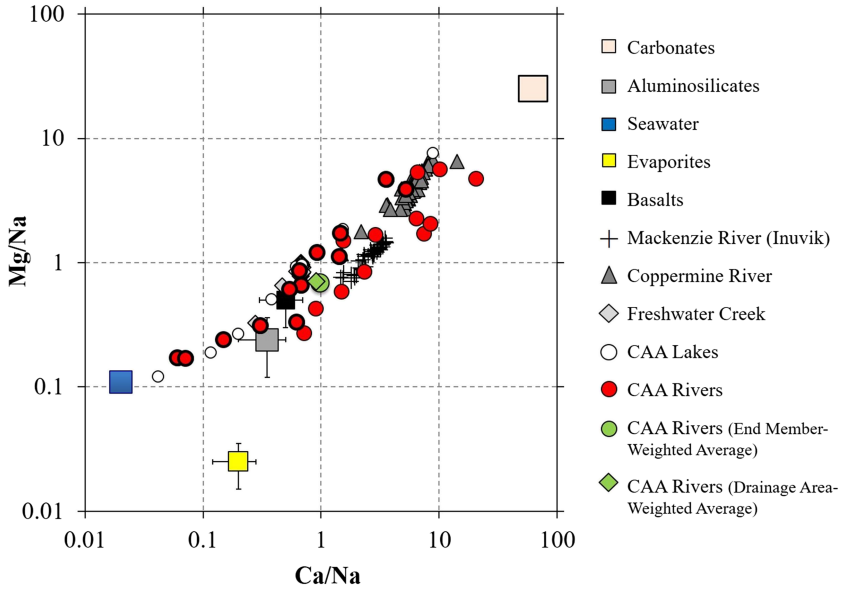

Figure 3. Major ion molar ratios from CAA rivers (red circles), lakes (white circles), and time-series data from the Coppermine River (gray triangles) and Freshwater Creek (gray diamonds) illustrate the imprint of drainage basin geology on dissolved ion concentrations. Most CAA samples fall along in a mixing line between waters draining silicate and carbonate bedrock end members. LSD rivers are distinguished from SFD rivers by a thick black outline (red circles with thick black outline). Average CAA river composition was determined using the end-member weighted (-EM, green circle) and area-weighted (-AW, green diamond) approaches described in section 2.7. Average bedrock end-member compositions after Gaillardet et al. (1999) and Millot et al. (2002). Mackenzie River time-series data are from the Arctic-GRO and PARTNERS programs (http://www.arcticgreatrivers.org/; dataset edition 20151021 with observations from June 2003 to June 2014). CAA River data are from Tables S2 and S3.

most cases ion concentrations remain invariant with measured discharge (diamonds, Figures 5 and S2). Discharge-weighted concentrations (annual averages, Table 2) and annual fluxes (Figure 6) of inorganic constituents were computed for each river's average number of flow days per year (365 and 143 days for the Coppermine River and Freshwater Creek, respectively). This analysis highlights differences in the annual average composition of these two rivers and differences in their baseline C-Q relationships, notably, Freshwater Creek has discharge-weighted concentrations of inorganic ions on the order of 1.5 to 45 times higher than the Coppermine River for all constituents except Ba (Table 2).

3.5. Scaling Observations to the Entire CAA

When scaled to the entire CAA, area-weighted major ion concentrations and average annual fluxes determined following the CAA-AW approach are as much as 8.5 times higher than estimates based on the CAA-EM extrapolation (Table 2 and Figure 6). This difference is likely caused by the disproportionate influence of the two largest rivers which account for 60% of the drainage area studied but just 10% of the CAA drainage region (Coppermine #16 and Back #26, Figure 4). This gives disproportionate weight to the major ion characteristics of these two large rivers once extrapolated, compared with the CAA-EM approach, which we consider more reliable (see section 4.2.1). Landscape variables such as bedrock geology and permafrost extent have been used in other studies to scale individual river geochemical observations to the broader CAA (Alkire et al., 2017; Li Yung Lung et al., 2018), lending more confidence to our CAA–EM approach.

4. Discussion

The following discussion illustrates that (1) although dissolved composition reflects gradients in landscape characteristics across the CAA, flow paths and residence time dictate river geochemical loads; therefore, (2) the geochemistry of small, costal draining CAA rivers can differ from the largest Arctic rivers that integrate various sources over a large, diverse landscape, which leads to the inference that, (3) these small

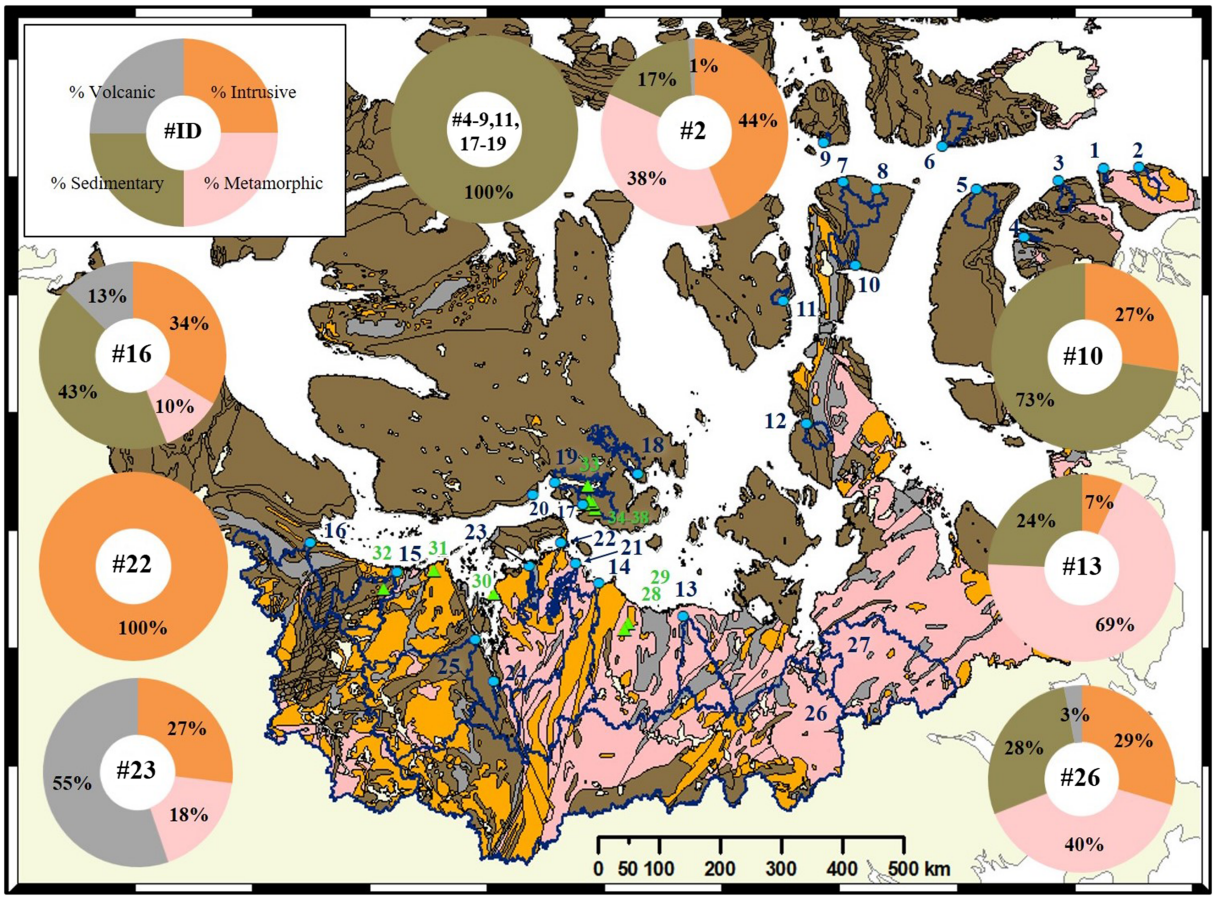

Figure 4. [Map] CAA-RP river sampling stations (blue circles), sampled lakes (green triangles), and drainage basin definitions (dark blue outline) for rivers listed in Figure 1. Dominant bedrock geology after Garrity and Soller (2009). [Circles around map] Bedrock lithology, % rocktype composition (outer circle), and river numerical ID (#ID) (inside circle) for most of the rivers sampled in this study. River #ID refers to locations/names as listed in Figure 1, Table S2.

coastal-draining rivers in the CAA will likely follow different, regionally specific trajectories of change compared with the largest Arctic rivers under a warming climate.

4.1. A Variety of River Flow Paths through the CAA Landscape Impact Inorganic Composition

Summer survey observations collected throughout the CAA illustrate the primary influence of two factors on regional river geochemistry: first, water source and connectivity (hydrology) and second, the composition of the drainage basin (bedrock geology). The CAA occupies a large, semicontinuous swath of islands from the Arctic Circle to the northern tip of Ellesmere Island, as such, gradients across this landscape are largely defined by S-N variation in temperature and geology. The southern CAA and high Arctic Islands are situated completely within the continuous permafrost zone (Hugelius et al., 2013), span five bioclimactic zones of terrestrial vegetative cover (CAVM, 2003), have some of the densest lake and watercourse coverage on the globe (Messager et al., 2016), and are littered with geomorphological evidence of glacial retreat after the last glacial maximum (Dyke, 2004). All of these landscape characteristics exert strong controls on river geochemical loads, contributing to spatially heterogeneous dissolved composition of CAA rivers.

4.1.1. Hydrological Influences on CAA River Geochemistry

Stable isotope observations from CAA rivers distinguish two types of hydrologic systems, one where direct input of snowmelt (or precipitation) dominates, and another where storage of water within the drainage basin (either in lakes, ponds, or vegetative cover) modifies water isotopic signatures, pulling them away from the average GMWL (Figure 2a). We have termed these two types of systems "surface flow" dominated (SFD) and "lake storage" dominated (LSD), respectively. The close association between the GMWL and our observations from small catchments in the northern CAA (river #s 1–8) indicates that these systems were

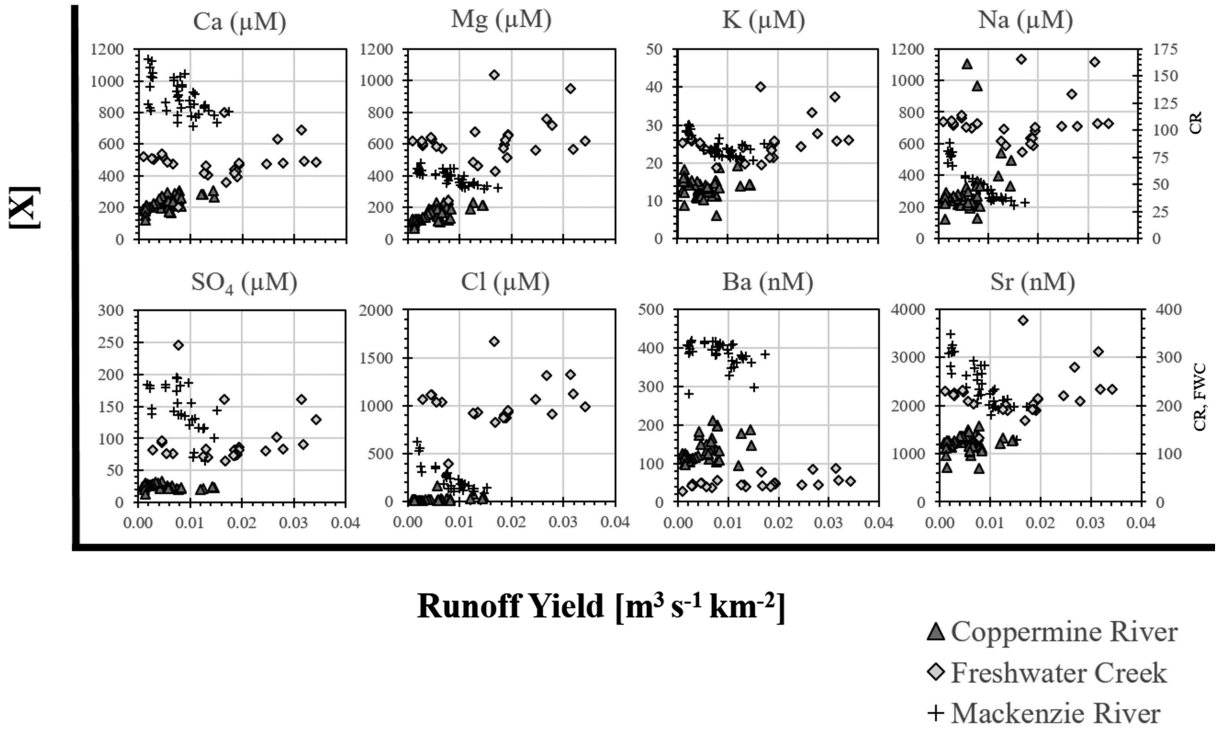

Figure 5. Measured major ion concentration versus runoff yield (daily average discharge/drainage basin area) for the Coppermine River (2014–2016), Freshwater Creek (2014–2016), and the Mackenzie River (2003–2014). Coppermine River observations combine data from Alkire et al. (2017) and this study (Table S3); Freshwater Creek time-series observations are from this study (Table S3), and the Mackenzie River time-series data are from Arctic-GRO and PARTNERS projects (http://www.arcticgreatrivers.org/; dataset edition 20151021 with observations from June 2003 to June 2014). Plots of Na and Sr data show the Coppermine River (CR) and Freshwater Creek (FWC) on the secondary Y-axes.

Table 2
LOADEST-Modeled Discharge-Weighted Annual Average Major and Minor Ion Concentrations and Isotope Values for the Coppermine River, Freshwater Creek, and the "Big 6" Arctic Rivers Based on Annual Time-Series Observations.

	Coppermine River[a]	Freshwater Creek[a]	Kolyma[b]	Lena[b]	Mackenzie[b]	Ob'[b]	Yenisei[b]	Yukon[b]	CAA-EM[d]	CAA-AW[e]
Major ions (μM)										
Ca	241	491	279	386	878	395	448	772	465	767
Mg	175	629	98	186	394	172	158	303	320	611
Na	50	769	66	392	336	276	281	115	470	803
K	16	26	15.9[c]	17.1[c]	23.5[c]	27.8[c]	16.5[c]	31.9[c]	19	75
SO_4	25	111	35	42	164	26	32	107	84	178
Cl	23	1,056	8.9	494	284	154	276	26	586	948
Minor ions (nM)										
Sr	123	216	611	1,289	2,159	1,138	1,514	1,444	752	1,071
Ba	136	54	63[f]	104[f]	371[f]	141[f]	76[f]	369[f]	44	376
Isotopes (‰)										
$\delta^{18}O$-H_2O	−19.5	−18.3	−22.2[f]	−20.5[f]	−19.2[f]	−14.9[f]	−18.4[f]	−20.2[f]	−18.3	−19.7

Note. CAA (-EM, -AW) estimates based on extrapolations from CAA rivers in Table S2.
[a]Daily LOADEST-modeled ion concentrations were averaged over the 3 years of observations (2014–2016) for the Coppermine River to generate an annual mean; because of the short open-water period for Freshwater Creek, monthly averages of LOADEST model ion concentrations were used to determine the annual mean (see section 2.6). [b]Daily LOADEST-modeled ion concentrations for Arctic-GRO rivers were determined for the period 2000-2009 by Tank et al. (2012). Daily averages were discharge-weighted using data from the Arctic-GRO edition 20151021 and then an annual average was computed for the modeled interval (see section 2.6). [c]Following Tank et al. (2012), LOADEST-modeled K concentrations were determined from observations made during the PARTNERS program from 2003 to 2006, daily average concentrations were then computed for the period 2000–2009. Daily averages were discharge-weighted using data from the Arctic-GRO edition 20151021 and then an annual average was computed for the modeled interval (see section 2.6). [d]CAA annual average concentrations were estimated using the "end-member" drainage basin method (section 2.7.1). *Note,* the intersection of the bedrock geology map (Garrity & Soller, 2009) and the Hydro-1k drainage area definitions misses about 5% of the total CAA drainage region (intersection = 1,401,690 km^2 vs. 1,471,410 km^2), so for consistency we have chosen to scale to the region of overlap only. [e]CAA annual average concentrations were estimated using the "area-weighted" drainage basin method (section 2.7.2), with the same caveats as in d (see note). [f]Discharge-weighted average data from the Arctic-GRO and PARTNERS program (2003–2006, 2007) as reported by Cooper et al. (2008), their table 1.

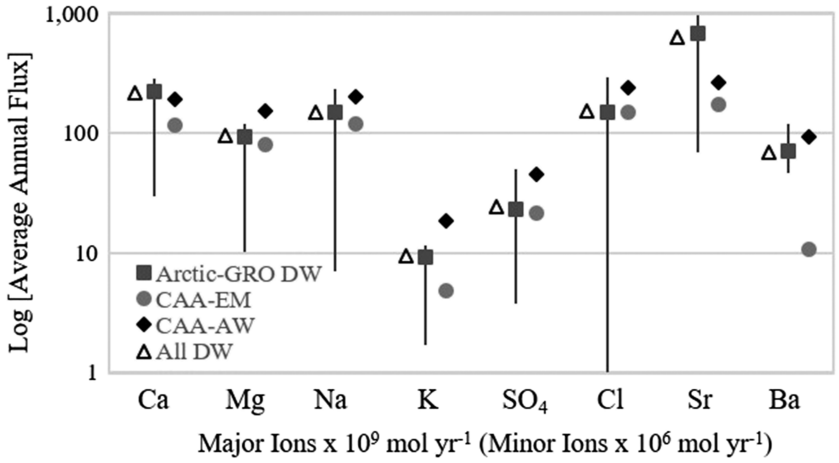

Figure 6. Mean annual fluxes of ions from the major pan-Arctic watersheds. Vertical lines indicate the spread (maxima and minima) of LOADEST-modeled constituent flux determinations for individual Arctic-GRO rivers (2000–2009) from Tank et al. (2012). Points on and adjacent to each line illustrate the discharge-weighted average annual mean flux for Arctic-GRO rivers (squares), the discharge-weighted estimates for the CAA drainage region alone (-EM, circle; -AW, diamond), and a discharge-weighted average flux determined using all the data (Arctic-GRO + average CAA estimates; triangles).

dominated by direct inputs of snowmelt or precipitation (as rain) at the time of sampling. These waters appear to have undergone little isotopic modification from their atmospheric sources (average *d-excess* = 7 ± 3; GMWL *d-excess* ≈ 10), though changes in relative humidity experienced as the snow pack ages could account for some deviation from the GMWL (e.g., Gibson et al., 2005; Taylor et al., 2001). Stable isotopic values in central CAA rivers (#9–12) were offset from the CMWL compared with the more northern samples (#1–8) but intermediate compared with rivers in the south (Figure 2a). This offset may be explained, in part, by a transition in the development of soils and vegetative cover moving from north to south that could facilitate intermediate storage of water (increased residence time) within the drainage system on longer time scales (e.g., CAVM, 2003). None of the rivers sampled in the north and central CAA (open circles, #1–12, Figure 2a) had large lakes within their drainage basins (all lakes were <4.2 km^2), and the proportion of lake cover was less than 2% for all of these systems (Table S2), reinforcing stable isotope observations. We have categorized these northern and central CAA rivers (#1–12) as being SFD systems.

Stable isotope ratios of rivers in the southern CAA (filled circles, Figure 2a), which include time-series observations from the Coppermine River and Freshwater Creek (triangles and diamonds respectively, Figure 2a), deviate from SFD rivers and the GMWL. These rivers have isotopic signatures characterized by evaporative loss, which decouples $\delta^{18}O$ and $\delta^{2}H$ and creates data arrays with slopes shallower than the GMWL (Edwards et al., 2004). Much lower *d-excess* of these southern CAA rivers (average *d-excess* = -1 ± 1) may reflect the influence of atmospheric distillation cycles as moisture travels inland or evaporative loss associated with storage in lakes within the drainage system (e.g., Froehlich et al., 2002; Gibson, 2002). All of these watersheds have lake cover of greater than 10% (up to 36%, Table S2) and drain some of the largest lakes in the CAA, including Takiyuak Lake, Point Lake, and Lac de Gras (Coppermine River), Ferguson Lake (Ekalluk River), and Contwoyto Lake (Burnside River). We have categorized these southern CAA rivers as being LSD systems. Lakes sampled in this study were, on average, more enriched in oxygen-18 and deuterium (isotopically heavier) than sampled rivers, indicating that further modification within the watershed is also impacting river discharges (e.g., mixing with other water sources). Even though appreciable groundwater inputs are not anticipated due to the presence of continuous permafrost in the region, the isotopic signature of infiltrating subsurface waters would be expected to generally reflect precipitation source, albeit with some modification due to mixing with surface waters, different residence times, interaction with solids, etc. (Gibson et al., 2005). This indicates that contributions from subsurface infiltrating waters or those associated with talik (thawed ground) formations below lakes within the drainage basin cannot be ruled out (Dugan et al., 2012; Gibson et al., 2005), especially in the southern CAA; however, this input would likely be

confined to the warmer seasons. In addition, the transition from drier tundra on mineral soils (Bioclimatic subzone C; CAVM, 2003) drained by central CAA rivers (#9–12) to moist tundra with more developed organic soils (Bioclimatic subzone D; CAVM, 2003) to the south may further contribute to increasing the residence time of water within the landscape.

One caveat to the above interpretation is the seasonal timing of sample collection. Available Environment Canada gauge data show a pronounced southwest to northeast progression in peak discharge for drainage regions across the CAA (not shown). Consequently, river samples collected in the north and central CAA were collected earlier relative to the seasonal progression and may have been more strongly affected by snowmelt. Rivers sampled in the southern CAA, collected later in the seasonal progression, are likely more influenced by lake flow and/or subsurface flow as the active layer deepens during the receding limb of the hydrograph. Time-series samples collected in the Coppermine River and Freshwater Creek clearly illustrate the seasonal shift in dominant freshwater source (Figure 2b). These two rivers follow the classic seasonal trajectory of Arctic freshwater systems, where surface and below ground input pathways are cut off and evaporation limited through the winter season, when isotopically light precipitation is stored in the snow pack (Edwards et al., 2004). As spring advances, snowmelt rapidly contributes a pulse of isotopically light runoff into the drainage system, dominating the signal while the ground is still frozen; once ice cover disappears and the soil thaw begins, seasonal evaporation of lake-stored waters and contributions from waters interacting with the deepening soil active layer begin to dominate the river signal (Edwards et al., 2004; Gibson et al., 2005).

4.1.2. Geologic Influences on CAA River Geochemistry

The CAA includes a uniquely ancient geologic region of the planet. As part of North America's Laurentia Craton, one of the world's oldest and largest assemblages of continental crust, the CAA is underlain by Canadian Precambrian shield formed by the collision of Archean crust and Proterozoic island arcs during the Early Proterozoic (2.5–1.6 Ga; Hoffman, 1988). Two dominant rock assemblages exist: much of the bedrock within the CAA originated during the Precambrian (>541 Ma); the Arctic Platform, however, is capped by much younger, Paleozoic sedimentary deposits of dolostones, limestones, shales, and sandstones (Trettin et al., 1991). Proterozoic collisions of a variety of crustal provinces resulted in the interleaving of numerous bedrock lithologies and ages in close proximity to each other (Garrity & Soller, 2009; Hoffman, 1988). For the rivers sampled in this study, this translates into distinct geologic composition within each drainage basin, particularly for rivers draining the continent along the southern (older) reach of the study area (Figure 4) and into a corresponding diversity of major ion compositions (Figure 3).

CAA river cation concentrations reflect this geologic diversity in the drainage systems sampled and loosely group along an “upper” and a “lower” mixing line between carbonate and silicate end members in Mg/Na-Ca/Na coordinates (Figure 3). The offset between these trends can be viewed through two different lenses: changes in Mg at constant Ca/Na, changes in Ca at constant Mg/Na, or a combination thereof. Drainage basin bedrock composition lends a partial explanation for this spread in the cation ratios, as the lower mixing line is dominated by rivers located in the north and central CAA that are underlain primarily by sedimentary bedrock, whereas rivers in the south, which are underlain by a mix of sedimentary and shield lithologies, dominate the upper mixing line (Table S2).

Higher Ca concentrations in north and central CAA rivers falling on the lower mixing line are readily explained by a higher proportion of sedimentary bedrock in their watersheds, shifting dissolved composition to higher Ca/Na at constant Mg; however, several rivers within the southern CAA also drain sedimentary bedrock. North-south gradients in surficial geology may explain some of the observed differences in Mg/Na-Ca/Na composition of sedimentary draining rivers that cause them to diverge from a single mixing line. Southern drainage basins, that dominate the upper mixing line, are characterized by greater percentage cover of glacial sediments, whereas more weathered bedrock and regolith characterizes many of the central CAA rivers (Mecham, Cunningham, Devon, and Garnier rivers). Differing composition of these glacial till sedimentary deposits, such as Mg-rich dolomites, could explain the higher Mg concentrations measured in the few southern rivers that exclusively drain sedimentary bedrock (Victoria Island rivers: Ekalluk, Jayko, Freshwater Creek; Table S2). Southern systems are also dominated by lakes (LSD systems) and may be further impacted by within-lake processes that modify major ion composition. Calcium carbonate is the major buffering complex of Arctic and sub-Arctic freshwaters, as such calcium carbonate hard water lakes have been observed to dominate the non-Precambrian bedrock regions of the CAA (Hamilton et al.,

2001). The deposition of $CaCO_3$-rich biogenic material or inorganic carbonate deposition within lakes would thus lower dissolved Ca concentrations, lowering Ca/Na ratios in the lakes and in the rivers draining them and potentially contributing to the separation of mixing lines in Figure 3.

4.1.3. Landscape-scale Influences on CAA River Geochemistry

The combined influence of water source and connectivity (hydrology) and drainage basin composition (bedrock geology) on CAA river geochemistry are intrinsically linked through the glacial history of this region. All the rivers sampled in this study drain landscapes that can be generally characterized as glaciated, lowland (<300 m above sea level), continuous permafrost regions with no appreciable peatlands (Smith et al., 2007, their figure 2). These types of previously glaciated landscapes are prime locations for lake formation because of glacial processes that acted to reduce landscape relief, create bedrock depressions, scour previous drainage systems, and drop low-permeability tills and ice blocks, promoting kettling (Smith et al., 2007). Combined with the geologic setting (e.g., faults, fractures, and lithology), and the presence of permafrost, these remnant features from repeated glaciations explain why lakes and ponds are a near-ubiquitous feature of the Canadian north (Pienitz et al., 2008).

The CAA itself is characterized by a strong gradient in lake cover, which decreases from south to north (r^2 = 0.55) and west to east (r^2 = 0.61; Table S2), and is further illustrated by our SFD (<2% lake cover; north and central CAA) and LSD (>10% lake cover; southern CAA) river categories. As discussed above, bedrock geology is also distributed with a S-N bias, with ancient Precambrian shield dominating in the south and younger sedimentary deposits dominating in the central CAA (section 4.1.2, Figure 4). The decreased occurrence of lakes to the north is coupled with a transition in the dominant landscape physiography, from glacial tills and exposed bedrock in the south, to weathered regolith in the central and northern CAA (Table S2). When plotted against location (latitude and longitude as independent variables), the presence of exposed bedrock (>75% rock outcrops) within sampled watersheds tended to decrease from south to north (r^2 = 0.39) and west to east (r^2 = 0.27). Although not well correlated, these trends in bedrock exposure follow gradients in lake cover (above), with lower % lake cover generally corresponding to regions of less exposed bedrock.

These coinciding gradients in lake cover fraction and surficial geology combine to influence river geochemical signatures across the CAA. LSD rivers dominate the "upper" mixing line in Figure 3 (symbols with thicker outline), whereas the "lower" mixing line is dominated by SFD rivers, indicating a role for water storage (residence time) in determining river geochemical composition. SFD systems of the north and central CAA directly deliver the weathering products of sedimentary carbonate rocks to the ocean, whereas LSD rivers in the south have more opportunity for geochemical loads to be altered through prolonged interaction with glacial tills and exposed Precambrian bedrock as waters are stored in lake systems, before delivering silicate weathering products (e.g., Na) to the ocean. But what significance does this have for our understanding of these systems in the future? While the physiographic features of the landscape are essentially static over the relevant timescale of years and decades, the presence and nature of lakes is not. In fact, lakes in permafrost regions across the pan-Arctic are changing (Smith et al., 2005). Regional warming trends have been linked to an increase in surface ponding, leading to the development of thermokarst and lake expansion in continuous permafrost regions. As permafrost degrades further, however, regions of discontinuous and sporadic permafrost have succumbed to lake drainage and eventual loss (Smith et al., 2005). Although it is not clear how much lake expansion or loss will occur in southern CAA watersheds underlain by Precambrian shield, thermokarst landscapes are present in the central CAA (e.g., Olefeldt et al., 2016), and the characteristics by which shield lakes fill and drain will be impacted by changing hydrological cycles (e.g., Spence & Woo, 2003, 2006). It is anticipated that a northward migration of the discontinuous permafrost zone across the pan-Arctic will result in the initial expansion of lake cover, followed by losses (Smith et al., 2007). This would be expected to impact both the storage of freshwater in CAA drainage basins as well as its geochemical processing and composition, ultimately impacting what dissolved constituents are delivered to the coastal ocean.

4.1.4. Implications of Changing Pathways for River Inorganic Geochemical Loads

An accelerated hydrological cycle and shifted seasonality of a warmer future Arctic is projected to result in as much as a 50% increase in river discharge by 2090, and a disproportionate amount of this increase will be felt north of the Arctic circle (Bring et al., 2017), thus coincident with the region dominated by medium and small Arctic rivers (e.g., Alkire et al., 2017; Holmes et al., 2002). Such alterations to freshwater delivery and cycles will ultimately modify how these drainage systems store, cycle, and release freshwater from the

terrestrial system to the ocean. Observations across the CAA indicate that differences in the pathways waters take through (and residence time within) the landscape lead to different constituents delivered to the ocean. A more deeply penetrating permafrost active layer due to higher summer temperatures will potentially result in enhanced storage of water within small SFD-type drainage systems, disproportionately located in the central and northern CAA, and ultimately increase the timescales of freshwater storage and release. A consequence of this is that stable isotope composition of SFD-type systems would tend toward those more characteristic of LSD-type rivers. Further, SFD-type systems experience more sedimentary carbonate bedrock weathering, thus differentiating them even further from LSD-type rivers draining the Precambrian shield in the south.

As warming progresses, physical and thermal disturbances of the permafrost active layer can expose soluble-ion-rich sediments, creating new opportunities for soluble ions to be accessed by infiltrating water (Frey & McClelland, 2009; Kokelj & Burn, 2005; Lamhonwah et al., 2017). These impacts would be felt in both SFD- and LSD-type systems, though might become more prominent in SFD-type systems if the retention time of water in the drainage system increases. Deepening of the permafrost active layer could result in increased flushing of Ca (and other constituents) into CAA rivers, as has been observed elsewhere (e.g., Keller et al., 2010; Lamhonwah et al., 2017; Roberts et al., 2017). Our observations within the north and central CAA may already be reflecting this process in SFD rivers, as shown by the "lower" mixing line in Figure 3. Fresh exposure of glacial sediments containing both carbonates and silicates has been shown to experience accelerated carbonate weathering, imparting a stronger effect of carbonate dissolution on stream geochemistry as flow paths deepen (Keller et al., 2010, and references therein), which may further explain the observed higher Ca concentrations in these systems. Based on work by Zhang et al. (2012, 2013) in other southern areas of the Canadian Arctic, seasonal thaw depth in the southern CAA can be expected to vary with vegetation cover, aspect, and elevation; as such, active layers may already extend to the bedrock in these systems if tills are shallow. In addition, the prevalence of wetlands may restrict active layer deepening where peat layers prevent further soil thaw. In either case, further warming may not enhance the mobilization of soluble ions if the active layer has already been stripped and a new reservoir of ions is not accessible from the underlying permafrost (e.g., Kokelj & Burn, 2005). Furthermore, rainfall events can provide intermittent but significant water sources to both LSD and SFD catchments after the snowmelt season, contributing to further flushing of ions from the deepening active layer (e.g., Lamhonwah et al., 2017; Lewis et al., 2012) or by enhancing the contributing area for runoff late in the season (Spence et al., 2015; Spence & Woo, 2006). The projected trend of increased precipitation in the north and central CAA will enhance precipitation in late autumn and winter (e.g., Bintanja & Selten, 2014; Bring et al., 2016), implying this mechanism will become more important in the future.

4.2. Similarities and Differences between CAA Rivers and the Large Arctic Rivers

4.2.1. Similarities to Large Arctic Rivers: Scaling Inorganic Composition

Time-series observations collected at the Coppermine River and Freshwater Creek lend context for regional scaling, assuming that these systems are representative of the entire CAA. This assumption is justified from a geological perspective as one river drains the Precambrian shield (Coppermine R.) and one the Paleozoic sedimentary deposits (Freshwater Creek), both of which dominate the broader CAA drainage (Figure 4). Poorly correlated concentration(C)-discharge(Q) relationships for most constituents in Freshwater Creek and some constituents in the Coppermine River (Figures 5 and S2) lend additional confidence to the estimation of average annual fluxes based on the extrapolation of summer survey values for these small river systems; however, these observations of weak C-Q relationships could be due to the limitations of our short time series, as other small coastal-draining rivers have been shown to have more tightly coupled C-Q relationships (discussed below).

From these extrapolations, annual average dissolved concentrations estimated using the CAA-EM approach fall within the range of the "Big 6" Arctic rivers for all ions except Na and Cl (Table 2). Since this approach scales to geology, it is not impacted by the same large-basin bias as the CAA-AW approach, likely making it a more reliable scaling method in such a geologically diverse region. Area-weighted ion concentration estimates (CAA-AW) are typically higher than those determined for the "Big 6" rivers (Table 2); in particular, Mg, Na, K, and Cl, which are estimated to be almost double the highest discharge-weighted values in the "Big 6" rivers. As discussed previously (section 3.5), the CAA-AW approach likely suffers from the so-

called "Amazon effect" (Meybeck, 1988), whereby the two largest rivers sampled are given disproportionate weight in the scaled average, as they account for 60% of the drainage area sampled but only 10% of the CAA drainage region.

Estimated average annual land-ocean fluxes from CAA rivers correspond more closely to the major Arctic rivers, with CAA-EM estimated fluxes always lower than those determined using the CAA-AW approach (Figure 6). Notably, average annual fluxes of K, Mg, Na, SO_4, and Cl, estimated with either method, fall to the high end of the "Big 6" ranges, whereas Ba and Sr fluxes tend towards the low end (vertical lines, Figure 6), with the CAA-EM Ba flux less than a quarter of that of the lowest "Big 6" rivers. Generally, estimated CAA ion fluxes bracket the discharge-weighted average values from the "Big 6" rivers (squares, Figure 6) and nudge these average fluxes slightly lower when combined into a pan-Arctic discharge-weighted average flux (triangles, Figure 6). While CAA fluxes are only estimated with sparse data, it is instructive to note that they do not deviate appreciably from the average fluxes of the major six Arctic river systems. This implies that an extrapolation of river characteristics of the "Big 6" would sufficiently reproduce the average major and minor ion fluxes for the CAA region and potentially the ungauged systems of the broader pan-Arctic system; however, this would not be the case for the extrapolation of water isotope ($\delta^{18}O$, $\delta^{2}H$) values, which overlap (Table 2), but are latitudinally dependent.

4.2.2. Differences from Large Arctic Rivers: Concentration-Discharge Relationships

The basic analysis presented above shows that extrapolating observations from the largest Arctic rivers to the undersampled regions of the Arctic (e.g., the CAA) may adequately characterize present day average *inorganic* fluxes to the Arctic Ocean. However, this same approach is not likely suitable for *organic* loads (e.g., Li Yung Lung et al., 2018), nor will it adequately predict the pan-Arctic response to future warming, as the small coastal systems of the CAA may follow different trajectories of change.

Time-series observations from the largest Arctic rivers indicate that inorganic ion concentrations (C) tend to decrease with increasing discharge (Q; e.g., Holmes et al., 2012; Ibarra et al., 2017), following a typical dilution model (e.g., Godsey et al., 2009; Figure S2). These same strongly negative C-Q relationships were not seen in the Coppermine River or Freshwater Creek observations made during this study nor in the longer time series of Environment Canada (EC) data presented by Li Yung Lung et al. (2018; not shown). With the exception of the Hornaday River, which exhibited strong (logC vs. logQ, $r^2 > 0.5$) negative C-Q relationships much like the Mackenzie River, other CAA rivers included in the EC data set showed only weak ($r^2 < 0.05$) negative C-Q relationships (Back, Burnside, and Ellice rivers, not shown; Li Yung Lung et al., 2018). Time series of dissolved ion concentrations measured in Freshwater Creek during our study more closely followed a typical chemostat relationship when plotted against Q, where C is relatively constant as Q changes (e.g., Godsey et al., 2009; Figure S2). Several constituents measured in the Coppermine River also demonstrated chemostat-like behavior (K, SO_4, Sr), whereas others showed positive (Ca, Na, Cl, Ba) and strongly positive (Mg) C-Q relationships over the time series (Figure S2). These observations suggest differences in transport versus source limitation for some constituents between the Coppermine River and Freshwater Creek catchments but also competing processes regulating inorganic ion mobilization within the same catchment. Positive slope C-Q relationships may reflect mobilization of reservoirs of easily mobilizable ions (e.g., soil and sediment pore spaces and thin films on mineral grains) that have been isolated since the last flushing and are accessed with the progressive deepening of the active layer. Alternatively, they may result from a dominance of atmospheric sources (e.g., Na, Cl, SO_4) or relate to more biologically active ions (e.g., K) that are leached from the thawing active layer at high flow (Walling & Webb, 1986). An increase in reactive surface area (reaction rates) with increased discharge has also been hypothesized as a mechanism to explain similar positive slope C-Q relationships in U.S. continental rivers (Godsey et al., 2009).

For the Coppermine River and Freshwater Creek, which both drain watersheds underlain by continuous permafrost, zero or positive slope C-Q relationships may track the evolution of the permafrost active layer as the warming season advances. If discharge is proportional to reactive surface area accessed by flow paths in southern river systems (Godsey et al., 2009), late-summer rain events accessing a much deeper permafrost active layer (i.e., increased reactive surface area) could skew major ion C-Q relationships towards more positive slopes. Incidentally, 2015 and 2016 were two such years where late season spikes in Coppermine River discharge were evident in early October and November, respectively. Continued high-resolution time-series observations of CAA rivers will be needed to capture these intermittent events and determine which C-Q

models best characterize these systems. Unusual C-Q relationships further indicate that land-ocean geochemical fluxes from small, coastal-draining CAA river systems may be controlled by processes unique to the region, both presently and in the future.

5. Conclusions: Uncertain Trajectories for Small, Coastal-draining CAA Rivers

The CAA is a geologically heterogeneous and complex region of the high Arctic whose diverse bedrock and hydrological settings are reflected in the geochemistry of its numerous small rivers. In the north and central CAA, river drainage basins are generally smaller, underlain by sedimentary bedrock, and their hydrology is driven by seasonal precipitation pulses that undergo little modification before they enter the coastal ocean. In the southern CAA, a high density of lakes stores water within the terrestrial realm for longer, permitting further modification of water isotope and geochemical characteristics. These larger southern CAA systems also transect through more geologically complex, ancient metamorphic, and intrusive bedrock that shapes their dissolved ion composition, potentially making their characteristics useful tracers for ecosystem studies.

Extrapolating observations of the largest Arctic rivers to the entire Arctic drainage system has shortcomings. While the major ion composition of CAA rivers in this study was generally similar to that of largest Arctic river systems, concentration-discharge relationships are notably different. Given that projected changes in hydrology and temperature across the Arctic will substantially affect the coastal regions, the role that smaller, coastal-draining rivers play in exporting land-derived inorganic ions to the Arctic Ocean will likely increase relative to the contributions from the "Big 6," wherein inorganic ion concentrations are diluted as discharge increases. This is a particularly important consideration for estimating inorganic fluxes to the narrow, shallow marine straits of the CAA, and potentially, to the Arctic outflow in the North Atlantic. Improved time-series sampling of both large and small river systems will greatly advance our understanding of the impact of terrestrial hydrology on the Arctic Ocean. Broad scale collaborations with an international network of northern partners (governments, community organizations, nongovernmental organizations, and universities) is indispensable in generating the necessary spatial coverage and long-term data sets to quantify and track change in these sensitive regions and to predict their future response.

Acknowledgments
This work was only possible through a network of enthusiastic and devoted collaborators. Partners included Polar Knowledge Canada and the Canadian High Arctic Research Station, the Arctic Research Foundation, the Kugluktuk Angoniatit Association, and the Canadian Arctic GEOTRACES Program. We acknowledge support from the Department of Fisheries and Oceans Canada, the Woods Hole Oceanographic Institution Coastal Ocean Institute, The G. Unger Vetlesen Foundation, Jane and James Orr, and the Woods Hole Research Center. Many thanks go to Austin Maniyogena, Angulalik Pedersen, Adrian Schimnowski, JS Moore, Les Harris, Oksana Schimnowski, as well as Barbara Adjun, Amanda Dumond, and Johnny Nivingalok, and the captains and crew of the research vessels CCGS Amundsen and R/V Martin Bergmann, all of whom supported our research and helped with sample collection. Special thanks also go to Valier Galy, Zhaohui "Aleck" Wang, Marty Davelaar, Michiyo Yamamoto-Kawai, Hugh McLean, Mike Dempsey, Baba Pedersen, Maureen Soon, Katherine Hoering, Sean Sylva, Ekaterina Bulygina, and Anya Suslova for their invaluable contributions during field program planning, preparations, and laboratory analyses. Robert Max Holmes is thanked for many fruitful discussions. We also thank several anonymous reviewers for their helpful comments on the paper's content and structure. All of the data presented in this paper can be found at https://doi.org/10.1594/PANGAEA.908497.

References

Alkire, M. B., Jacobson, A. D., Lehn, G. O., Macdonald, R. W., & Rossi, M. W. (2017). On the geochemical heterogeneity of rivers draining into the straits and channels of the Canadian Arctic Archipelago. *Journal of Geophysical Research: Biogeosciences*, *122*, 2527–2547. http://doi.org/10.1002/2016JG003723

Bintanja, R., & Selten, F. M. (2014). Future increases in Arctic precipitation linked to local evaporation and sea-ice retreat. *Nature*, *509*(7501), 479–482. http://doi.org/10.1038/nature13259

Booth, G., Raymond, P., & Oh, N.-H. (2007). LoadRunner v. 1.2b, Yale University, New Haven, CT, https://environment.yale.edu/loadrunner/

Bring, A., & Destouni, G. (2009). Hydrological and hydrochemical observation status in the pan-Arctic drainage basin. *Polar Research*, *28*, 327–338.

Bring, A., Fedorova, I., Dibike, Y., Hinzman, L., Mård, J., Mernild, S. H., et al. (2016). Arctic terrestrial hydrology: A synthesis of processes, regional effects, and research challenges. *Journal of Geophysical Research: Biogeosciences*, *121*, 621–649. http://doi.org/10.1002/2015JG003131

Bring, A., Shiklomanov, A., & Lammers, R. B. (2017). Pan-Arctic river discharge: Prioritizing monitoring of future. *Earth's Future*, *5*, 72–92. http://doi.org/10.1002/eft2.175

Carmack, E. C., Yamamoto-Kawai, M., Haine, T. W. N., Bacon, S., Bluhm, B. A., Lique, C., et al. (2016). Freshwater and its role in the Arctic Marine System: Sources, disposition, storage, export, and physical and biogeochemical consequences in the Arctic and global oceans. *Journal of Geophysical Research: Biogeosciences*, *121*, 675–717. http://doi.org/10.1002/2015JG003140

CAVM (2003). Circumpolar Arctic Vegetation Map. (1: 7,500,000 scale), Conservation of Arctic flora and fauna (CAFF) Map No. 1. U.S. Fish and Wildlife Service, Anchorage, Alaska. http://www.ArcticAtlas.org/

Clark, I. D., & Fritz, P. (1997). *Environmental isotopes in hydrology* (p. 328). Boca Raton, Florida, USA: CRC Press/Lewis Publishers.

Cohn, T. A. (1988). Adjusted maximum likelihood estimation of the moments of lognormal populations from type I censored samples, In: U.S. Geological Survey Open-File Report 88-350, 34 p.

Cohn, T. A., Gilroy, E.J., & Baier, W.G. (1992). Estimating fluvial transport of trace constituents using a regression model with data subject to censoring, In: Proceedings of the Joint Statistical Meeting, Boston, August 9–13, 1992, p. 142–151

Cooper, L. W., McClelland, J. W., Holmes, R. M., Raymond, P. A., Gibson, J. J., Guay, C. K., & Peterson, B. J. (2008). Flow-weighted values of runoff tracers ($\delta^{18}O$, DOC, Ba, Alkalinity) from the six largest Arctic rivers. *Geophysical Research Letters*, *35*, L18606. http://doi.org/10.1029/2008GL035007

Dansgaard, W. (1964). Stable isotopes in precipitation. *Tellus*, *16*(4), 436–468. http://doi.org/10.3402/tellusa.v16i4.8993

Dickson, A. G. (1990). Standard potential of the reaction: AgCl(s) + 1/2H (g) = Ag (s) + HCl (aq), and and the standard acidity constant of the ion HSO_4^- in synthetic sea water from 273.15 to 318.15 K. *Journal of Chemical Thermodynamics*, *22*, 113–127.

Dickson, A. G., Sabine, C. L., & Christian, J. R. (Eds) (2007). *Guide to best practices for ocean CO_2 measurements*, *PICES Special Publication*, (Vol. 3, p. 191). Sidney, BC, Canada: PICES. Sidney, BC, Canada.

Dittmar, T., & Kattner, G. (2003). The biogeochemistry of the river and shelf ecosystem of the Arctic Ocean: A review. *Marine Chemistry*, *83*(3–4), 103–120. http://doi.org/10.1016/S0304-4203(03)00105-1

Doxaran, D., Devred, E., & Babin, M. (2015). A 50% increase in the mass of terrestrial particles delivered by the Mackenzie River into the Beaufort Sea (Canadian Arctic Ocean) over the last 10 years. *Biogeosciences*, *12*(11), 3551–3565. http://doi.org/10.5194/bg-12-3551-2015

Dugan, H. A., Gleeson, T., Lamoureux, S.F., & Novakowski, K. (2012). Tracing groundwater discharge in a High Arctic lake using radon-222. *Environmental Earth Sciences*, *66*, 1385–1392.

Dyke, A. S. (2004). An outline of North American deglaciation with emphasis on central and northern Canada. In J. Ehlers & P. L. Gibbard (Eds.), *Developments in Quaternary Sciences* (Vol. 2, Part B, pp. 373–424). San Diego, CA: Elsevier.

Edwards, T. W. D., Wolfe, B. B., Gibson, J. J., & Hammarlund, D. (2004). Use of water isotope tracers in high latitude hydrology and paleohydrology. In R. Pienitz, M. S. V. Douglas, & J. P. Smol (Eds.), *Long-term environmental change in the Arctic and Antarctic lakes* (pp. 187–207). Netherlands: Springer.

Frey, K. E., & McClelland, J. W. (2009). Impacts of permafrost degradation on Arctic river biogeochemistry. *Hydrological Processes*, *23*(1), 169–182. http://doi.org/10.1002/hyp.7196

Froehlich, K., Gibson, J., & Aggarwal, P. (2002). Deuterium excess in precipitation and its climatological significance. In *Study of environmental change using isotope techniques* (Vol. C&S Paper (pp. 54–66). Vienna, Austria: International Atomic Energy Agency.

Gaillardet, J., Dupré, B., Louvat, P., & Allègre, C. J. (1999). Global silicate weathering and CO_2 consumption rates deduced from the chemistry of large rivers. *Chemical Geology*, *159*(1–4), 3–30. http://doi.org/https://doi.org/10.1016/S0009-2541(99)00031-5

Garrity, C. P., & Soller, D. R. (2009). Database of the Geologic Map of North America — Adapted from the Map by J.C. Reed, Jr. and Others, 2005. *U.S. Geological Survey Data Series*, *424*. USGS, Denver, CO, USA. https://pubs.usgs.gov/ds/424/

Geological Survey of Canada, (2014). Surficial geology of Canada; Geological Survey of Canada, Canadian Geoscience Map 195 (preliminary, Surficial Data Model v. 2.0 conversion of Map 1880A), scale 1:5 000 000. doi:https://doi.org/10.4095/295462

Gibson, J. J. (2002). Short-term evaporation and water budget comparisons in shallow Arctic lakes using non-steady isotope mass balance. *Journal of Hydrology*, *264*, 242–261.

Gibson, J. J., Edwards, T. W. D., Birks, S. J., St Amour, N. A., Buhay, W. M., McEachern, P., et al. (2005). Progress in isotope tracer hydrology in Canada. *Hydrololgical Processes*, *19*(1), 303–327. http://doi.org/10.1002/hyp.5766

Godsey, S. E., Kirchner, J. W., & Clow, D. W. (2009). Concentration-discharge relationships reflect chemisatic characteristics of US catchments. *Hydrological Processes*, *23*, 1844–1864.

Haine, T. W. N., Curry, B., Gerdes, R., Hansen, E., Karcher, M., Lee, C., et al. (2015). Arctic freshwater export: Status, mechanisms, and prospects. *Global and Planetary Change*, *125*, 13–35. http://doi.org/10.1016/j.gloplacha.2014.11.013

Hamilton, P. B., Gajewski, K., Atkinson, D. E., & Lean, D. R. S. (2001). Physical and chemical limnology of 204 lakes from the Canadian Arctic Archipelago. *Hydrobiologia*, *457*, 133–148. http://doi.org/10.1023/A:1012275316543

Hoffman, P. F. (1988). United Plates of America, the birth of a craton: Early Proterozoic assembly and growth of Laurentia. *Annual Review of Earth and Planetary Sciences*, *16*, 543–603.

Holmes, R. M., Coe, M. T., Fiske, G. J., Gurtovaya, T., McClelland, J. W., Shiklomanov, A. I., et al. (2013). Climate change impacts on the hydrology and biogeochemistry of Arctic rivers. In: C. R. Goldman, M. Kumagai, & R. D. Robarts (Eds.), *Climatic change and global warming of inland waters: Impacts and mitigation for ecosystems and societies* (First, pp. 1–26). Chichester, West Sussex, UKJohn Wiley & Sons. http://doi.org/10.1002/9781118470596.ch1

Holmes, R. M., McClelland, J. W., Peterson, B. J., Raymond, P. A., Tank, S. E., Zhulidov, A. V., (2011). River Biogeochemistry. Arctic Report Card: Update for 2011.

Holmes, R. M., McClelland, J. W., Peterson, B. J., Shiklomanov, I. A., Shiklomanov, A. I., Zhulidov, A. V., et al. (2002). A circumpolar perspective on fluvial sediment flux to the Arctic ocean. *Global Biogeochemical Cycles*, *16*(4), 1098. http://doi.org/10.1029/2001GB001849

Holmes, R. M., McClelland, J. W., Peterson, B. J., Tank, S. E., Bulygina, E., Eglinton, T. I., et al. (2012). Seasonal and annual fluxes of nutrients and organic matter from large rivers to the Arctic Ocean and surrounding seas. *Estuaries and Coasts*, *35*(2), 369–382. http://doi.org/10.1007/s12237-011-9386-6

Holmes, R. M., McClelland, J. W., Raymond, P. A., Frazer, B. B., Peterson, B. J., & Stieglitz, M. (2008). Lability of DOC transported by Alaskan rivers to the Arctic Ocean. *Geophysical Research Letters*, *35*, L03402. https://doi.org/10.1029/2007GL032837

Holmes, R. M., Peterson, B. J., Gordeev, V. V., Zhulidov, A. V., Meybeck, M., Lammers, R. B., & Vörösmarty, C. J. (2000). Flux of nutrients from Russian rivers to the Arctic Ocean: Can we establish a baseline against which to judge future changes? *Water Resources Research*, *36*(8), 2309. http://doi.org/10.1029/2000WR900099

Hugelius, G., Tarnocai, C., Broll, G., Canadell, J. G., Kuhry, P., & Swanson, D. K. (2013). The northern circumpolar soil carbon database: Spatially distributed datasets of soil coverage and soil carbon storage in the northern permafrost regions. *Earth System Science Data*, *5*(1), 3–13. http://doi.org/10.5194/essd-5-3-2013

HYDAT (2016). Environment Canada Data Explorer V2.1.7, 2010-2016, Environment Canada—Water Survey of Canada HYDAT Version: 1.0 (Oct 16, 2017), http://www.ec.gc.ca/rhc-wsc

Ibarra, D. E., Moon, S., Caves, J. K., Chamberlain, C. P., & Maher, K. (2017). Concentration–discharge patterns of weathering products from global rivers. *Acta Geochimica*, *36*(3), 405–409. http://doi.org/10.1007/s11631-017-0177-z

IUPAC (1997). Compendium of chemical terminology. In A. D. McNaught, & A. Wilkinson (Eds.), (2nd ed.). Oxford, U. K: Blackwell Sci. https://doi.org/10.1351/goldbook.P04758. [Available at, http://goldbook.iupac.org

Keller, K., Blum, J. D., & Kling, G. W. (2010). Stream geochemistry as an indicator of increasing permafrost thaw depth in an arctic watershed. *Chemical Geology*, *273*(1–2), 76–81. http://doi.org/10.1016/j.chemgeo.2010.02.013

Kokelj, S. V., & Burn, C. R. (2005). Geochemistry of the active layer and near-surface permafrost, Mackenzie delta region, Northwest Territories, Canada. *Canadian Journal of Earth Sciences*, *42*, 37–48.

Lafrenière, M., & Lamoureux, S. (2008). Seasonal dynamics of dissolved nitrogen exports from two High Arctic watersheds, Melville Island, Canada. *Hydrology Research*, *39*(4), 323. http://doi.org/10.2166/nh.2008.008

Lamhonwah, D., Lafreniere, M., Lamoureux, S. F., & Wolfe, B. B. (2017). Multi-year impacts of permafrost disturbance and thermal perturbation on High Arctic stream chemistry. *Arctic Science*, *3*(2), 254–276.

Lammers, R. B., Shiklomanov, A. I., Vörösmarty, C. J., Fekete, B. M., Peterson, B. J. (2016). R-ArcticNet, A regional hydrographic data network for the Pan-Arctic Region (ISO-image of CD-ROM). PANGAEA, https://doi.org/10.1594/PANGAEA.859422, website: http://www.r-arcticnet.sr.unh.edu/v4.0/index.html

Laudon, H., Spence, C., Buttle, J., Carey, S. K., McDonnell, J. J., McNamara, J. P., et al. (2017). Save northern high-latitude catchments. *Nature Geoscience*, *10*(5), 324–325. http://doi.org/10.1038/ngeo2947

Lewis, T., Lafrenière, M. J., & Lamoureux, S. F. (2012). Hydrochemical and sedimentary responses of paired High Arctic watersheds to unusual climate and permafrost disturbance, Cape Bounty, Melville Island, Canada. *Hydrological Processes*, *26*(13), 2003–2018. http://doi.org/10.1002/hyp.8335

Li Yung Lung, J. Y. S., Tank, S. E., Spence, C., Yang, D., Bonsal, B., McClelland, J. W., & Holmes, R. M. (2018). Seasonal and geographic variation in dissolved carbon biogeochemistry of rivers draining to the Canadian Arctic Ocean and Hudson Bay. *Journal of Geophysical Reserach-Biogeosciences*, *123*, 3371–3386. https://doi.org/10.1029/2018JG004659

Mann, P. J., Davydova, A., Zimov, N., Spencer, R. G. M., Davydov, S., Bulygina, E., et al. (2012). Controls on the composition and lability of dissolved organic matter in Siberia's Kolyma River basin. *Journal of Geophysical Reserach*, *117*, G01028. https://doi.org/10.1029/2011JG001798

McClelland, J. W., Déry, S. J., Peterson, B. J., Holmes, R. M., & Wood, E. F. (2006). A pan-arctic evaluation of changes in river discharge during the latter half of the 20th century. *Geophysical Research Letters*, *33*, L06715. http://doi.org/10.1029/2006GL025753

McClelland, J. W., Holmes, R. M., Peterson, B. J., Amon, R., Brabets, T., Cooper, L., et al. (2008). Development of a pan-Arctic database for river chemistry. *Eos, Transactions of the American Geophysical Union*, *112*(G4), 217–218. http://doi.org/10.1029/2006JG000353

McClelland, J. W., Holmes, R. M., Peterson, B. J., & Stieglitz, M. (2004). Increasing river discharge in the Eurasian Arctic: Consideration of dams, permafrost thaw, and fires as potential agents of change. *Journal of Geophysical Research*, *109*, D18102. http://doi.org/10.1029/2004JD004583

McClelland, J. W., Townsend-Small, A., Holmes, R. M., Pan, F., Stieglitz, M., Khosh, M., & Peterson, B. J. (2014). River export of nutrients and organic matter from the North Slope of Alaska to the Beaufort Sea. *Water Resources Research*, *50*, 1823–1839. https://doi.org/10.1002/2013WR014722

McLaughlin, F. A., Carmack, E. C., Ingram, R. G., Williams, W. J., & Michel, C. (2006). Oceanography of the Northwest Passage. In *The sea: Ideas and observations on the progress in the study of seas, Vol. 14, Part B: The global coastal ocean, interdisciplinary regional studies and syntheses* (Chap. 31, pp. 1211–1242). Cambridge, MA: Harvard University Press.

McLaughlin, F. A., Proshutinsky, A., Carmack, E. C., Shimada, K., Brown, K., Corkum, M., et al. (2012). Physical, chemical, and zooplankton data from the Canada basin and Canadian Arctic Archipelago, July 20 to September 14, 2006. *Canadian Data Report of Hydrography and Ocean Sciences*, *186*, 373p. Retrieved from http://www.dfo-mpo.gc.ca/Library/346783.pdf

Messager, M. L., Lehner, B., Grill, G., Nedeva, I., & Schmitt, O. (2016). Estimating the volume and age of water stored in global lakes using a geo-statistical approach. *Nature Communications*, *7*, 1–11. http://doi.org/10.1038/ncomms13603

Meybeck, M. (1988). How to establish and use world budgets of riverine materials. In A. Lerman, & M. Meybeck (Eds.), *Physical and Chemical Weather in Geochemical Cycles* (pp. 247–272). Norwell, MA: Kluwer Academic Publishers.

Millero, F. J. (1979). The thermodynamics of the carbonate system in seawater. *Geochimica et Cosmochimica Acta*, *43*(10), 1651–1661.

Millot, R., Gaillardet, J., Dupré, B., & Allègre, C. J. (2002). The global control of silicate weathering rates and the coupling with physical erosion: New insights from rivers of the Canadian Shield. *Earth and Planetary Science Letters*, *196*(1–2), 83–98. http://doi.org/10.1016/S0012-821X(01)00599-4

Olefeldt, D., Goswami, S., Grosse, G., Hayes, D., Hugelius, G., Kuhry, P., et al. (2016). Circumpolar distribution and carbon storage of thermokarst landscapes. *Nature Communications*, *7*(1), 13043. https://doi.org/10.1038/ncomms13043

Peterson, B., Holmes, R., McClelland, J., Vorosmarty, C., Lammers, R., Shiklomanov, I., & Rahmstorf, S. (2002). Increasing river dischange to the Arctic Ocean. *Science*, *298*(13), 2171–2173. http://doi.org/10.1126/science.1077445

Peterson, B., Holmes, R. M., McClelland, J., Tank, S. E., Raymond, P., Striegl, R., & Shiklomanov, A. (2016). Arctic Great Rivers Observatory I Biogeochemistry Data (2009-2011). *Arctic Data Center*. https://doi.org/10.18739/A2ZQ03.

Peterson, B. J., McClelland, J., Curry, R., Holmes, R. M., Walsh, J. E., & Aagaard, K. (2006). Trajectory shifts in the Arctic and subarctic freshwater cycle. *Science*, *313*(5790), 1061–1066. https://doi.org/10.1126/science.1122593

Peucker-Ehrenbrink, B., & Miller, M. W. (2003). Quantitative bedrock geology of Alaska and Canada. *Geochemistry, Geophysics, Geosystems*, *4*(4), 8005. http://doi.org/10.1029/2002GC000449

Peucker-Ehrenbrink, B., & Miller, M. W. (2007). Quantitative bedrock geology of the continents and largescale drainage regions. *Geochemistry, Geophysics, Geosystems*, *8*, Q06009. http://doi.org/10.1029/2006GC001544

Pienitz, R., Doran, P. T., & Lamoureux, S. F. (2008). Origin and geomorphology of lakes in the polar regions. In W. F. Vincent, & J. Laybourn-Parry (Eds.), *Polar lakes and rivers: Limnology of Arctic and Antarctic aquatic ecosystems* (pp. 25–32). UK: Oxford University Press.

Pierrot, D., Lewis, E., & Wallace, D. W. R. (2006). MS Excel program developed for CO_2 system calculations, ORNL/CDIAC-105a, Carbon Dioxide Inf. Anal. Cent., Oak Ridge Natl. Lab., U.S. Dep. of Energy, Oak Ridge, Tenn., doi:https://doi.org/10.3334/CDIAC/otg.CO2SYS_XLS_CDIAC105a.

Prowse, T. D., & Flegg, P. O. (2000). The magnitude of river flow to the Arctic Ocean: Dependence on contributing area. *Hydrological Processes*, *14*, 3185–3188. http://doi.org/10.1002/1099-1085(200011/12)14:16/17<3185::AID-HYP170>3.0.CO;2-S

Roberts, K. E., Lamoureux, S. F., Kyser, T. K., Muir, D. C. G., Lafrenière, M. J., Iqaluk, D., et al. (2017). Climate and permafrost effects on the chemistry and ecosystems of High Arctic Lakes. *Scientific Reports*, *7*(1), 1–8. http://doi.org/10.1038/s41598-017-13658-9

Romanovsky, V.E., Smith, S. L., Christiansen, H. H., Shiklomanov, N. I., Streletskiy, D.A., Drozdov, D. S., et al. (2013). Permafrost. In: Arctic Report Card: Update for 2013, http://www.arctic.noaa.gov/report13/permafrost.html

Runkle, R. L., Crawford, C. G., & Cohn, T. A. (2004). Load estimator (LOADEST): A FORTRAN program for estimating constituent loads in streams and rivers. In *U.S. Geol. Surv. Tech. and Meth.,* Book 4 (Chap. A5, pp. 1–69. U.S. Geol., Surv., Denver, Co.

Schuur, E., Bockheim, J., & Canadell, J. (2008). Vulnerability of permafrost carbon to climate change: Implications for the global carbon cycle. *BioScience*, *58*(8), 701. http://doi.org/10.1641/B580807

Schuur, E. A. G., McGuire, A. D., Schädel, C., Grosse, G., Harden, J. W., Hayes, D. J., et al. (2015). Climate change and the permafrost carbon feedback. *Nature*, *520*(7546), 171–179. http://doi.org/10.1038/nature14338

Shadwick, E. H., Thomas, H., Gratton, Y., Leong, D., Moore, S. A., Papakyriakou, T., & Prowe, A. E. F. (2011). Export of Pacific carbon through the Arctic Archipelago to the North Atlantic. *Continental Shelf Research*, *31*(7–8), 806–816. http://doi.org/10.1016/j.csr.2011.01.014

Shevchenko, V. P., Dolotov, Y. S., Filatov, N. N., Alexeeva, T. N., Filippov, A. S., Nothig, E.-M., et al. (2005) Biogeochemistry of the Kem' River estuary, White Sea (Russia). *Hydrology and Earth System Sciences*, *9*, 57–66.

Smith, L. C., Sheng, Y., & MacDonald, G. M. (2007). A first pan-Arctic assessment of the influence of glaciation, permafrost, topography and peatlands on northern hemisphere lake distribution. *Permafrost and Periglacial Processes*, *18*, 201–208.

Smith, L. C., Sheng, Y., MacDonald, G. M., & Hinzman, L. D. (2005). Disappearing arctic lakes. *Science*, *308*(5727), 1429. https://doi.org/10.1126/science.1108142

Spence, C., Kokelj, S. V., Kokelj, S. A., McCluskie, M., & Hedstrom, N. (2015). Evidence of a change in water chemistry in Canada's subarctic assocatied with enhanced winter streamflow. *Journal of Geophysical Research Biogescinces*, *120*, 113–127. https://doi.org/10.1002/2014JG002809

Spence, C., & Woo, M.-K. (2003). Hydrology of subarctic Canadian Shield: Soil-filled valleys. *Journal of Hydrology*, *279*, 151–166.

Spence, C., & Woo, M.-K. (2006). Hydrology of subarctic Canadian Shield: Heterogeneous headwater basins. *Journal of Hydrology*, *317*, 138–154.

Tank, S. E., Raymond, P. A., Striegl, R. G., McClelland, J. W., Holmes, R. M., Fiske, G. J., & Peterson, B. J. (2012). A land-to-ocean perspective on the magnitude, source and implication of DIC flux from major Arctic rivers to the Arctic Ocean. *Global Biogeochemical Cycles*, *26*, GB4018. http://doi.org/10.1029/2011GB004192

Taylor, S., Feng, X., Kirchner, J. W., Osterhuber, R., Klaue, B., & Renshaw, C. E. (2001). Isotopic evolution of a seasonal snowpack and its melt. *Water Resources Research*, *37*(3), 759–769. http://doi.org/10.1029/2000WR900341

Trettin, H. P., Mayr, V., Long, G. D. F., & Packard, J. J. (1991). Cambrian to Early Devonian basin development sedimentation and volcanism, Arctic Islands: Chapter 8. In H. P. Trettin (Ed.), *Geology of the Innuilian Orogen and Arctic Platform of Canada and Greenland*, *Geology of Canada* (Vol. 3, pp. 163–238). Vancouver, BC, CA: Geological Survey of Canada. . https://doi.org/10.1130/DNAG-GNA-E

Uppström, L. R. (1974). The boron/chlorinity ratio of deep-sea water from the Pacific Ocean. *Deep Sea Research and Oceanographic Abstracts*, *21*(2), 161–162. http://doi.org/10.1016/0011-7471(74)90074-6

Voss, B. M., Peucker-Ehrenbrink, B., Eglinton, T. I., Fiske, G., Wang, Z. A., Hoering, K. A., et al. (2014). Tracing river chemistry in space and time: Dissolved inorganic constituents of the Fraser River, Canada. *Geochimica et Cosmochimica Acta*, *124*, 283–308. http://doi.org/10.1016/j.gca.2013.09.006

Walling, D. E., & Webb, B. W. (1986). Solutes in river systems, Chapter 7. In S. T. Trudgill (Ed.), *Solute processes* (pp. 251–327). Toronto: John Wiley & Sons.

White, D., Hinzman, L., Alessa, L., Cassano, J., Chambers, M., Falkner, K., et al. (2007). The Arctic freshwater system: Changes and impacts. *Journal of Geophysical Research*, *112*, G04S54. http://doi.org/10.1029/2006JGO00353

Zhang, Y., Chen, W., & Riseborough, D. W. (2008). Transient projections of permafrost distribution in Canada during the 21st century under scenarios of climate change. *Global and Planetary Change*, *60*(3–4), 443–456. http://doi.org/10.1016/j.gloplacha.2007.05.003

Zhang, Y., Li, J., Wang, X., Chen, W., Sladen, W., Dyke, L., et al. (2012). Modelling and mapping permafrost at high spatial resolution in Wapusk National Park, Hudson Bay Lowlands. *Canadian Journal of Earth Sciences*, *49*(8), 925–937. https://doi.org/10.1139/e2012-031

Zhang, Y., Wang, X., Fraser, R., Olthof, I., Chen, W., McLennan, D., et al. (2013). Modelling and mapping climate change impacts on permafrost at high spatial resolution for an Arctic region with complex terrain. *The Cryosphere*, *7*(4), 1121–1137. https://doi.org/10.5194/tc-7-1121-2013

References From the Supporting Information

Lammers, R. B., Shiklomanov, A. I., Vörösmarty, C. J., Fekete, B. M., & Peterson, B. J. (2001). Assessment of contemporary Arctic river runoff based on observational discharge records. *Journal of Geophysical Research*, *106*, 3321. http://doi.org/10.1029/2000JD900444

Vuglinsky, V. S. (1997). River water in flow to the Arctic Ocean—Conditions of formation, time variability and forecasts. In K. Aagaard, D. Hartmann, V. Kattsov, D. Martinson, R. Stewart, & A. Weaver (Eds.), *Proceedings of the ACSTS Conference on Polar Processes and Global Climate, Rosario, Orcas Island, WA, USA, 3–6 November 1997* (Vol. 2, pp. 277–278). International ACSYS Project Office: Oslo.

Walker, E. R. (1977). Aspects of oceanography in the archipelago. Report 52633 for the Department of Fisheries and Oceans Canada, Institute of Ocean Sciences, Patricia Bay Sidney, B.C., Retrieved from https://doi.wiley.com/10.1029/2010GC003372